

Draft 11 December 1995

in Press

Revised for Limnology and Oceanography

Appendix 4

The 1991 coccolithophore bloom in the central north Atlantic

I. Optical properties and factors affecting their distribution

William M. Balch

Bigelow Laboratory for Ocean Sciences, McKown Point, West Boothbay Harbor, ME
04575

Katherine A. Kilpatrick

Division of Meteorology and Physical Oceanography, Rosenstiel School for Marine and
Atmospheric Science, University of Miami, 4600 Rickenbacker Causeway, Miami, FL
33149-1098

Charles C. Trees

Center for Hydro-Optics and Remote Sensing, San Diego State University, 6505 Alvarado
Rd., Suite 206, San Diego, CA, 92182

Running head- Coccolithophore bio-optics

Acknowledgements

Derek Harbour kindly provided phytoplankton taxonomic information. The officers and crew of the RRS Charles Darwin are acknowledged for their expert ship handling and the staff of the Research Vessel Services, Barry, U.K. are thanked for their support of the ship studies. Don Heuer helped with the figures. Patrick Holligan provided considerable logistical support and helped with data interpretation along with Emilio Fernandez. The AVHRR data were provided by P.E. Baylis at the Satellite Receiving Station, University of Dundee, U.K. Some of the beam attenuation data used to calculate total scatter were kindly provided by Roy Lowry of the British Oceanographic Data Centre, Bidston, U.K. Howard Gordon and Kenneth Voss (Univ. of Miami Physics Dept.) have provided help in data interpretation. Two anonymous reviewers provided valuable comments on an earlier version of this manuscript. This work was generously supported by ONR Ocean Optics Program (N00014-91-J-1048), NASA Global Biogeochemistry (NAGW 2426) and NSF Biological Oceanography Program (OCE-8900189 and OCE-9022227) to WMB. This paper is contribution ### to the U.S. Global Ocean Flux Program.

Abstract

Optical scatter and absorption were measured in the central north Atlantic Ocean during a mesoscale bloom of the coccolithophorid, *Emiliania huxleyi*. The chlorophyll-specific absorption was similar to previously reported measurements of the same species in laboratory cultures. Suspended coccoliths were responsible for about 80% of the total backscattering in the center of the bloom and the greatest calcite-dependent backscattering was observed just below the base of the mixed layer. Areal maps of calcite-dependent backscattering and reflectance were similar, due to the dominance of backscatter over absorption. Calculated reflectance at 440 and 550 nm reached about 24%, slightly less than what has been observed previously in Gulf of Maine blooms. Total scattering (b) was also calculated as the difference between beam attenuation and absorption. The ratio \tilde{b}_b (backscattering divided by total scatter) was about 0.01-0.02 at 440 nm and 550 nm at the most turbid parts of the coccolithophore bloom ($b = 1 - 3 \text{ m}^{-1}$). As total scattering decreased below 1 m^{-1} , \tilde{b}_b increased. The behavior of \tilde{b}_b was compared for coccolith-dominated versus chlorophyll-dominated waters. Vertical profiles of calcite-dependent scattering, combined with satellite remote sensing data, were used to assess the factors responsible for vertical transport of calcite. The subsurface peak in calcite-dependent scattering did not result from detached coccoliths sinking but resulted either from plated coccolithophores sinking, then detaching their plates, or from deep coccolithophores producing and detaching their plates *in situ*.

Introduction

Coccolithophores are members of the algal class Prymnesiophyceae (Green et al. 1990). These cells produce calcium carbonate scales called coccoliths which, when released from the cells, increase its turbidity. They are known as an important part of the organic and calcite carbon production in the north Atlantic (Lohmann 1920; Hentschel 1936; Halldal 1953 as cited by Braarud 1963). Their optical properties have been the subject of considerable attention since the discovery that these organisms produce meso-scale blooms, observable by satellite (Holligan et al. 1983; Aiken and Bellan 1990, Balch et al. 1991; Trees et al. 1992; Fukushima and Ishizaka 1993; Brown and Yoder 1993). Satellite data withstanding, observations of turbid coccolithophore blooms have been made before. Birkenes and Braarud (1952) recorded turbid blooms of *Emiliania huxleyi* in Norwegian fjords. Anecdotal evidence of white-water blooms in the three major ocean basins can be found in Brongersma-Saunders (1957) although in some cases, bacteria have also been implicated (Lapota et al. 1988). Nevertheless, references to "milky" blooms caused by coccolithophores are fairly common. Berge (1962) cited a bloom in 1955 in F rdesfjord, Norway with coccolith concentrations of $115,000 \text{ mL}^{-1}$ plus other observations dating back to 1911, while Braarud (1945) cited a bloom in August 1935 near other Norwegian fjords with coccolith concentrations of $33,500 \text{ mL}^{-1}$.

Turbidity in coccolithophore blooms is thought to be principally due to the light scattering properties of the algal cells and associated coccoliths (Ackleson et al. 1994) although the exact relationships remain poorly defined. By "scattering" we are referring to particle scattering (as opposed to Rayleigh scattering) where the wavelength of light is less than, or equal to, the particle size. Such light scattering is mainly in the forward direction (Hodkinson and Greenleaves 1963) and is size dependent; smaller particles have a smaller efficiency of scattering than do large particles. Particle scattering in most natural waters is dominated by particles greater than $2\mu\text{m}$ (Jerlov 1976). Light scattering of homogeneous spheres has been modeled (beginning with Mie 1908) but scattering by intricately shaped

particles like coccoliths, or by particles of varying refractive index, such as organic matter and calcite, is much more complex to solve analytically (Bricaud et al. 1992). The reader is referred to Kirk (1994) or Jerlov (1976) for excellent reviews of light scattering in the sea.

The scattering coefficient in the sea has often been related to chlorophyll concentration (Gordon and Morel 1983; Morel 1987) although it is well known that other types of biogenic particles scatter light (Morel and Ahn 1991). For example, Kitchen and Zaneveld (1990) observed vertical profiles of scatter that were significantly different from chlorophyll profiles. Suspended minerals also are thought to dominate the backscattering signal in certain areas (Brown and Gordon 1974) but the magnitude of the light scattering by minerals has been poorly understood in space and time. Given the ubiquitous distribution of coccolithophores in the world ocean, it is also likely that a significant amount of reflected light detected by satellite remote sensors is from calcite which may cause error in the remote determination of chlorophyll (Balch et al. 1989). Knowledge of the bio-optical properties of coccoliths are important for correction of remotely sensed pigment data.

Interestingly, there have been virtually no published laboratory studies of coccolithophore light scattering (this is currently ongoing in our laboratory) and one laboratory study on absorption by *E. huxleyi* (Morel and Bricaud 1981). The only observations of light scattering by coccolithophores are from a scant few field studies. This paucity of data is striking, given the importance of calcite to carbon sedimentation, burial, as well as its potential impact on water-leaving radiance, and the remote sensing of phytoplankton chlorophyll.

We have studied the optical properties of *E. huxleyi* in nature. There are three important constraints that affect the interpretation of field data. First, measurements must be made in situations dominated by coccolithophores, with minimal representation by other algal groups. Second, the growth dynamics of the populations must be well-documented because bio-optical properties of coccolithophores change as populations age and cells drop

their coccoliths (Balch et al. 1992, 1993). Third, the optical properties of the calcite must be separable from the properties of other organic and inorganic matter.

A meso-scale coccolithophore bloom formed south of Iceland during June-July of 1991 which met all of these requirements. The turbid bloom covered an area of about 0.5 million km², *E. huxleyi* was the dominant phytoplankton species. There was excellent satellite coverage from the beginning to the end of the bloom (about 3 weeks), so the growth dynamics were well documented in space and time (Holligan et al. 1993; Fernandez et al. 1993). We were able to separate the optical properties of calcite from organic matter by making measurements before and after calcite dissolution. This paper is the first of a two part series; part I summarizes the absorption, scattering and backscattering properties of this spectacular algal event and part II (Balch et al. submitted) relates these properties to the particle concentrations, as well as their size.

Methods

Observations were made on cruise 60 of the RRS Charles Darwin (CD60) from 13 June to 3 July, 1991. The cruise track is shown in figure 1. Two transects were made along the 20°W and 15°W meridian. Detailed vertical profiles of light scattering and absorption in the top 100-200 meters depth, were performed at 24 hydrographic stations (Table 1). One of the stations was close to an optics mooring at 59° 39' N x 20° 59' W. While steaming, underway surface samples were taken hourly for particle absorption, volume scattering, chlorophyll concentration, and beam attenuation. The concentration of suspended calcite, cell and coccolith counts also were measured but the relevance of these to the optical signal will be discussed in the second paper of this series (Balch et al. submitted). Other measurement details can be found in Holligan et al. (1993).

Pigment Concentration

Pigment measurements were made using the technique of Yentsch and Menzel (1963), modified by Holm-Hansen et al. (1965). A seawater sample of 200mL was

filtered onto Gelman GFF filters, then the pigment extracted overnight at 4°C in 10mL of 90% acetone. Fluorescence was measured with a Turner 111 fluorometer.

Volume Scattering Measurements

Samples for measuring volume scattering were collected from Niskin bottles and stored in polyethylene bottles prior to the measurements (which immediately followed the cast). Volume scattering is defined by Kirk (1994) as "the radiant intensity in a given direction from a volume element, dV , illuminated by a parallel beam of light, per unit of irradiance on the cross-section of the the volume, and per unit volume". Measurements of volume scattering were made with a Brice Phoenix model 2000 light scattering photometer (Brice et al. 1950). The reader is referred to Spilhaus (1965), and Pak (1970) for discussions on the accuracy and precision of the Brice Phoenix light scattering photometer when used with sea water samples. Each 30mL sample was placed in a 6-sided glass cuvette designed for sampling at 45°, 90° and 135°. Occasionally, samples were allowed to warm several degrees before making measurements to eliminate condensation on the cuvette windows. Replicate measurements made over 30 minutes of warming showed no effect on the volume scattering function. Calibration of the instrument was made with an opal glass reference and working standard supplied with the instrument. Calibration constants were checked routinely to determine the instrument's stability. Finally, distilled water blanks were run to verify instrument calibration and to check the absolute accuracy of the instrument. These consisted of 0.2µm-filtered distilled water from a Milli-Q system, and were run 27 times during the cruise. Dark current measurements were performed after every sample. During one experiment, volume scatter of a bottled sample was examined immediately and after 16.5h in a surface-cooled deck incubator to verify any containment effects. The 90° volume scatter decreased about 12% over 16.5h (about 0.7% per hour). Given that our samples were run immediately following a cast, and only 3 angles were measured, any containment effect would have been negligible. This is in

agreement with Spilhaus (1965) who demonstrated that containment effects were negligible provided storage time was ≤ 1 h (he took readings at 5° intervals between 30° and 135° thus sampling time was potentially longer).

Volume scattering of each seawater sample was measured at the three angles stated above and at two wavelengths (436 nm and 546 nm). Then the sample was bubbled for 30s with CO_2 (Paasche 1962) which reduced the pH to 5.0 and dissolved the calcium carbonate. Volume scattering measurements were repeated on the de-calcified samples. Cell counts were performed as a control to verify that the cell concentration was unaffected by the CO_2 bubbling and only the calcite dissolved. An Olympus BH2 microscope equipped with polarization optics and epifluorescence was used on board the ship for this purpose.

The technique of Gordon (1976) was used to calculate the backscattering coefficient (b_b , that fraction of light scattered in the backwards direction per unit thickness; See Table 2 for complete list of symbols used in this work). The method uses volume scattering at 45° , 90° , and 135° as input. Essentially, the input volume scattering data are fit to an analytic expression of Beardsley and Zaneveld (1969), and this function is integrated in the backwards direction to calculate the backscattering coefficient. The difference between the raw and the acidified backscattering was considered "calcite-dependent backscattering" (b_b').

Particulate Absorption Measurements

A reflectometer technique was used to measure the particulate absorption coefficient (a_p , the fraction of incident quanta that are absorbed per unit thickness of a material). A complete description of the technique, with comparisons to the spectrophotometric method, can be found in Balch and Kilpatrick (1992). One liter samples were filtered through baked Gelman GFF filters for particulate absorption measurements. The filters were stored in plastic petri dishes and frozen at -20°C for up to 3 days. Mitchell and Kiefer (1988) have

indicated that absorption spectra of filter pads with phytoplankton are stable at this temperature. Before analysis, a flat-black circular mask was placed over each filter to cover the clean white rim, free of particles. Spectral reflectance of each filter was measured every 10 nm between 400 and 700 nm using a hand-held Colormet spectral reflectometer (Instrumar Engineering Limited, St John's, Newfoundland, Canada). Absorbance was calculated based on the ratios of reflectance from sample and blank using the Kubelka-Munk function (Kubelka and Munk 1931 as cited in Kortüm 1969). The absorption coefficient is calculated using the clearance area of the filter, the volume filtered, and a path correction. Pigment-specific absorption coefficients are within 5% of those calculated using the spectrophotometric filter pad technique of Mitchell (1990) performed on the same samples, provided the optical densities of the filtered sample >0.3 (see Balch and Kilpatrick 1992; their Fig. 7). *In situ* absorption measurements were not available to compare to the filter pad measurements. No detrital correction was made for the particulate absorption, thus, a_p values may have been overestimated, although in the middle Atlantic, the concentration of colored dissolved organic matter is expected to be low. No correction was needed for coccolith absorption; it has been previously demonstrated in other coccolithophore blooms that coccoliths absorb negligible light between 400 and 700 nm (Balch et al. 1991; their Fig. 9).

Beam Attenuation Measurements and Scatter Calculations

Beam attenuation (fraction of a parallel light beam which is absorbed or scattered per unit pathlength) was measured using two beam transmissometers, a Sea Tech 0.25m pathlength transmissometer with a wavelength of 660 nm and the Scripps Vis Lab Spectral Transmissometer (VLST; Petzold and Austin 1968) with a folded 1 m pathlength. The model of Voss (1992) was first used to calculate c_{440} and c_{550} from measured values of c_{660} (Sea Tech) and c_{535} (VLST) respectively. Voss (1992; his Fig. 8) has tested and verified this model in a wide variety of water types, including coccolithophore blooms with

attenuation values $>1\text{m}^{-1}$. Following the correction of the data for wavelength, the differences in optical geometry were corrected according to Voss and Austin (1993). Voss (1992) and Voss and Austin (1993) should be consulted for complete details about the correction procedures.

Total scatter (b ; the integrated volume scattering function over all solid angles) was calculated as the difference between beam attenuation (c) and the sum of water absorption (a_w) and particulate absorption (a_p). Values of a_w were taken from Smith and Baker (1981).

Spectroradiometer Measurements

Measurements of radiance (quantum flux per unit solid angle) and irradiance (quantum flux on a surface normalized by area) were made with a Biospherical Instruments MER 1032 spectroradiometer. Data discussed in this work are for downwelling irradiance (410, 441, 488, 532, 550, 589, 633, 656, 671, and 694 nm), upwelling irradiance (410,441, 488, 520, 550, 589, 633, and 671nm), upwelling radiance (410,441, 488, 520, 550, 589, and 710nm), and scalar irradiance (PAR).

Results

The performance of the Brice Phoenix Light Scattering Photometer showed negligible drift in both calibration constants and distilled water checks over the period of this cruise. Distilled water blanks ($n=27$) were run over the two weeks and values were close to pure water values in absolute terms, and stable. Average volume scattering at 90° (β_{90}) was $2.99 \times 10^{-4} \text{ m}^{-1} \text{ sr}^{-1}$ at 436nm (standard deviation= 1.91×10^{-5} ; coefficient of variation= 6.5%) and $1.41 \times 10^{-4} \text{ m}^{-1} \text{ sr}^{-1}$ at 546nm (standard deviation= 1.89×10^{-5} ; coefficient of variation= 13.4%). Interpolated pure water values published by Jerlov (1976) were $2.527 \times 10^{-4} \text{ m}^{-1} \text{ sr}^{-1}$ at 436 nm and $0.9604 \times 10^{-4} \text{ m}^{-1} \text{ sr}^{-1}$ at 546nm; the reason the ship values were higher than pure water values is probably due to the difficulty in achieving

particle-free water aboard ship. The other measure of the stability of this instrument was the variation of the calibration coefficients. Calibration records are available for this particular instrument for the last 14.5 years, and show that between 1978 and 1993, using the same opal glass standard, the calibration coefficient at 436nm and 546nm decreased by 0.47% per year and 0.12% per year respectively. Thus, over the course of this 3 week cruise, instrument drift would have been negligible.

Volume scattering at 90° reached extremely high values within the north Atlantic coccolithophore bloom: $0.02 \text{ m}^{-1} \text{ sr}^{-1}$ at 440 nm and 550 nm which is about 70X and 165X the value of pure seawater at the respective wavelengths (Gordon et al. 1980). Over the entire North Atlantic study area, 90° volume scattering and backscattering were linearly related at both wavelengths, with the most variability in the relationship seen with the clearest water. The relationships relating backscattering to 90° volume scattering at 440 nm and 550 nm are given in Table 3. The least-squares fits were highly significant ($r^2 \geq 0.997$; $P(\text{Type 1}) < 0.1\%$; F statistics exceeding 55,000!).

The difference between raw and acidified backscatter (b_b') was almost always measurable. It should be noted that in samples where coccolithophores were absent, no significant change in scatter was observed upon bubbling with CO_2 . Some b_b' values of zero were observed in the southern portion of the study area, but negative values were rare, indicating that cell breakage was negligible.

Calcite-dependent backscattering represented over 70% of the total backscatter in vertical profiles and was highest within the top 40m. Below 40m, b_b' values were about 10-15% of the total backscattering at 440 nm and 550 nm (Fig. 2A and B). While the phytoplankton population was dominated by *E. huxleyi* in the high reflectance feature, non-calcareous species dominated outside the patch. However, two species of calcareous algae were found at $59^\circ 39' \text{ N} \times 20^\circ 59'$, outside the dense coccolithophore bloom, *Coccolithus pelagicus* (78 cells mL^{-1}) and *E. huxleyi* ($681 \text{ cells mL}^{-1}$) with a very low concentration of detached *E. huxleyi* coccoliths (9 mL^{-1}). *C. pelagicus* did not drop its

plates appreciably. Due to the large size of *C. pelagicus* cells, their calcite dominated the total suspended calcite. Even in this "non-bloom" station, about 25-33% of the total backscattering was due to calcite (b_b') down to 50m depth (Fig. 2C and D).

At all of the stations, both total backscattering and calcite-dependent backscattering showed well-defined wavelength dependence. Least squares linear fits for b_b 440 versus b_b 550 and b_b' 440 versus b_b' 550 are given in Table 3. These relationships translated to a wavelength dependence of $\lambda^{-1.212}$ for total backscatter and $\lambda^{-1.196}$ for calcite-dependent backscatter which was highly significant ($P=0.001$; F statistic >7000 ; $r^2 > 0.979$).

Chlorophyll (Chl) and particulate absorbance were positively correlated, although there was somewhat more variability than in the above scattering relationships ($P(\text{Type } 1) < 0.001$, F statistic = 648 and 273 and $r^2 = 0.721$ and 0.521 at 440 and 550 nm respectively; Table 3). Using these results, the value of a_p^*440 varied from 0.18 at the lowest chlorophyll concentrations to 0.078 at the upper chlorophyll concentrations. There was no significant covariation between a_p and b_b or a_p and b_b' .

Maps of surface a_p , b_b and b_b' at 440 nm and 550 nm allowed examination of the large-scale patchiness of these optical properties. Within the bloom, values of a_p 440 and a_p 550 were highest along the 15°W transect and in the far western part of the survey area between 22°W and 23°W. Lowest particulate absorbance values within the bloom were observed along the 20°W transect. Outside the bloom, the highest particulate absorption was observed at the shelf break off of the northwest coast of Ireland (Fig. 3A and B). Patterns of b_b and b_b' were very similar for both wavelengths; this was expected given that calcite backscattering represented at least 70% of the total backscattering in the bloom. Highest backscattering values were observed in the western part of the survey area (Fig. 3C,D,E, and F).

Vertical sections of a_p at 440 nm and 550 nm (Fig. 4A and B) showed greater absorbance at the northern part of the transect, with a peak between 58-58.5°N, similar to the chlorophyll pattern (Fernandez et al 1993) but outside of the region of maximum

turbidity. Below about 50 m, phytoplankton absorption generally declined. The vertical section of backscattering (Fig. 4C and D) showed greatest values at 61°N and at 25m depth. This same pattern was observed for the b_b' data (Fig. 4E and F), again suggesting that the backscattering in the surface water column was dominated by calcite-dependent scattering.

The beam attenuation data were first corrected for wavelength differences, then instrument differences. At 8 stations of the cruise, there were simultaneous transmittance measurements using both instruments. Uncorrected VLST transmittance (with water subtracted, cvl_{535}) was correlated to uncorrected ST transmittance (with water subtracted, cst_{660} ; Fig 5A; $r^2 = 0.97$) but the least squares fit to the data showed significantly higher beam attenuation of suspended material at 535 nm than 660 nm. After adjusting both to the same wavelength according to Voss (1992; see Fig. 5B for example of c corrected to 550 nm; $r^2 = 0.97$), the VLST still gave significantly larger beam attenuation values after water was subtracted. Following correction of the data for differences in optical geometry, the data fell considerably closer to the 1:1 line, although some deviation still was observed at low attenuation values (Fig. 5C; $r^2 = 0.97$). These results showed that the correction algorithms of Voss (1992) and Voss and Austin (1993) functioned adequately; henceforth, these algorithms were applied to all c measurements to make the data from the two transmissometers intercomparable.

Once beam attenuation results were tabulated, then total light scatter (b) was calculated as the difference between total beam attenuation and total absorption. Values of b reached as high as 3 m^{-1} in the center of the bloom. Due to the time-consuming nature of the measuring absorption and beam attenuation to calculate the scattering coefficient, we derived an empirical algorithm to conveniently estimate $b(\lambda)$ based on the easier measurement of $bb(\lambda)$:

$$b(\lambda) = b_{\max}(\lambda) \left[\frac{bb(\lambda) - bb_0(\lambda)}{Kb(\lambda) + (bb(\lambda) - bb_0(\lambda))} \right] \quad (7)$$

The parameter $b_{\max}(\lambda)$ represented the maximum scattering, $bb_0(\lambda)$ represented the lower limit of total backscattering, as $b(\lambda)$ approached clear water values, and $Kb(\lambda)$ represented the value of $bb(\lambda)$ when $b(\lambda)$ was one half its maximal value. The equation was iteratively solved at varying values of total backscattering and the results are given in Table 4 and Fig. 6. The same data were plotted showing the backscattering probability, $bb(\lambda)/b(\lambda)$ ($=\tilde{b}_b$) as a function of $b(\lambda)$ (Fig. 7). It can be seen that at $b(440)$ and $b(550)$ values of 1 m^{-1} , \tilde{b}_b was 0.01 to 0.02. Below 1 m^{-1} , \tilde{b}_b increased to high values of 0.3 at 440nm and 0.6 at 550 nm in the clearest ocean water but such high values are questionable as will be discussed later.

Discussion

Optical observations

Backscattering and the shape of the volume scattering function (VSF) were similar to previously described VSF's of coccolithophore blooms (Balch et al. 1991) as indicated by the ratio of bb/β_{90} . Pure seawater without particles should have a bb/β_{90} ratio of about 8 sr at 550nm (Gordon et al 1980). In clear water off the Bahamas, the bb/β_{90} ratio at 530nm was 6.67 while in the very turbid water of San Diego Harbor, the bb/β_{90} ratio was 4.16 (Petzold 1972). Clearly, as turbidity increases, the volume scattering function flattens in the backwards direction so that bb/β_{90} falls. The same was true in the mesoscale coccolithophore bloom studied here. Brice Phoenix measurements showed that β_{135} values generally were close to the β_{90} values when coccolith concentrations were highest (approaching a flat VSF in the backwards direction). Moreover, the least square fits to the backscattering versus volume scattering relationships (Table 3) gave bb/β_{90}

ratios of 5 sr (440nm) and 4 sr (550nm) when large numbers of suspended coccoliths were present. This can be compared to previously measured bb/β_{90} ratios of the 1989 coccolithophore bloom in the Gulf of Maine (Balch et al. 1991; their table 1, station 4) which were 4.3 sr (440 nm) and 5.9 sr (550 nm).

The North Atlantic bloom differed from the Gulf of Maine blooms in that the wavelength dependence of backscattering was less than published previously ($\lambda^{-1.19}$ as opposed to $\lambda^{-1.45}$; see Balch et al. 1991) but this should be interpreted cautiously since it is based on only two wavelengths. There also were two similarities between the aforementioned blooms. Water with high backscattering coefficients was confined to the top 20-30 m in the North Atlantic, as in the Gulf of Maine. Finally, in the Gulf of Maine, >75% of the backscatter was from coccoliths, similar to the North Atlantic bloom.

Regional variability of bio-optical properties

The aerial extent of the bloom was probably larger than indicated by the Advanced Very High Resolution Radiometer (AVHRR) imagery. In regions thought to be well outside the bloom, based on the satellite images, 1/3 of the backscattered light was still attributed to suspended calcite (Fig. 2C and D). The extent to which the bloom size was underestimated from the satellite images can be seen in Fig. 8 which shows b_b' overlaid on the AVHRR image of June 19, 1994. When this image was made (19 June, 1991; 1504 GMT), the ship was at about 60°N x 20°W and it can be seen that there was low reflectance in the satellite image yet there was measurable b_b' (Fig.8). Generally, the patterns of the high reflectance measured by the satellite agreed well with the patterns defined by the objective contouring of bb' . More important, though, is that there was measurable b_b' along the 20°W transect as far south as 55°N (500 km south of the first visible high reflectance water at 61°N;). Indeed, Holligan et al. (1993) reported concentrations of coccoliths of 5000-10,000 mL⁻¹ at 57°N. While there is no doubt that

the very high reflectance water extended from 61°N to 63°N, it should be kept in mind that *E. huxleyi* significantly impacted the optical properties of the water as far south as 55°N.

We predicted irradiance reflectance, R , of the surface water based on the measured values of a_p and b_b using equation 2 of Gordon et al. (1988):

$$R = Q * \sum_{i=1}^2 l_i * \{bb/(a+bb)\}^i \quad (2)$$

where l_1 and l_2 are empirically-fit coefficients equal to 0.0949 and 0.0794 respectively. Total absorption (a) was set equal to the sum of particulate absorption and water absorption. This model required knowledge of Q , the ratio of upwelling radiance to the upwelling irradiance toward zenith. Q equals π for a totally diffuse radiance distribution and increases with zenith angle. Average values of Q at 440 and 550 nm were 6.00 and 6.12 respectively and these values were used in all subsequent reflectance calculations (Table 5). Patterns of surface reflectance (Fig. 9) were remarkably similar to the patterns of bb' (Fig. 3E and 3F). Reflectance values predicted by equation 2 were as high as 21% at 440 nm and 24% at 550 nm in the northwest sector of the survey area. The predicted reflectance values at 440nm and 550nm were compared with values measured with the MER spectroradiometer. There were seven stations where this comparison was possible (Fig 10). At both wavelengths, the predicted irradiance reflectance accounted for 89% or 93% of the true variance in R_{440} and R_{550} , respectively. The standard error of the predicted reflectances based on these relationships is +/- 3.4% and 2.3% at 440nm and 550 nm respectively. For the comparison shown in Figure 10, the slopes were not significantly different than 1 nor were the intercepts significantly different from zero ($P(\text{Type 1}) < 0.05$). Such reflectance values are a bit lower than those measured with a spectroradiometer in the 1989 Gulf of Maine coccolithophore bloom (26.8% and 32.8%

respectively; Balch et al. 1991, their Table 1). It also should be noted that the ship crossed through a shelf-break coccolithophore bloom while returning to Scotland which can be seen in the southeast portions of the contour maps (Fig. 3).

The particulate absorption data allowed calculation of the chlorophyll-specific absorption coefficient of a coccolithophore population dominated by *E. huxleyi*. There were other species present such as cyanobacteria, naked dinoflagellates, and other miscellaneous eukaryotic microflagellates, thus while coccolithophores dominated the algal assemblage, it was not a pure population. The range of chlorophyll-specific absorption-- 0.098 to 0.14 m² mg chl⁻¹ at chlorophyll concentrations of 1.5 and 0.1 µg L⁻¹ respectively-- was similar to the range observed by others and is indicative of a package effect (Morel and Bricaud 1981; see also Yentsch and Phinney 1989; their Fig. 6). While the chlorophyll-specific absorption was high relative to non-coccolithophore species (Mitchell and Kiefer, 1988), the average ap^*_{440} in the most turbid part of the coccolithophore bloom was about 0.10 m² mg chl⁻¹, in good agreement with Morel and Bricaud (1981) who found ap^*_{440} of *E. huxleyi* cultures to be about 0.093 m² mg chl⁻¹. The ap^*_{440} values showed no significant correlation to b_b throughout the study area. Absorption at 440 nm was well correlated to chlorophyll biomass, but it is worthy of note that the high concentrations of coccoliths were not necessarily associated with the maximum chlorophyll biomass. In fact, along the 20°W transect, the largest 440 nm absorption (hence highest biomass; Fernandez et al. 1993) was observed at the edge of the high reflectance feature, not inside it (Fig. 3 and 4). This further supports the view that the term "bloom" is a misnomer with coccolithophores.

Variability in the ratio of backscatter to scatter

Clearly, in the North Atlantic coccolithophore event, scatter dominated absorption in terms of its impact on beam attenuation. Total scatter calculated from the difference between beam attenuation and absorption was as high as 3.3 m⁻¹ at 440 nm and 2.9 m⁻¹ at 550nm, almost 25-fold greater than the largest 440 nm absorption and 100-fold bigger

than 550 nm absorption observed in the bloom. The relation of total scatter to backscatter was highly nonlinear (Fig. 6), as would be expected since the forward part of the volume scatter function changes shape dramatically with increasing particle load. The volume scattering function of pure water is symmetrical which sets the upper value of \tilde{b}_b at 0.5. The same results in Fig. 6 were replotted (Fig. 7) to show the values of \tilde{b}_b as a function of b . It can be seen that in the most turbid parts of the bloom with $b > 1.0$, the value of \tilde{b}_b was about 0.01, regardless of wavelength. The most difficult region to calculate \tilde{b}_b (that is when \tilde{b}_b is changing most rapidly) is when b falls between 0 and 0.5 m^{-1} which also happens to be when absorption becomes a more important part of the total beam attenuation. Note that measured \tilde{b}_b values approached the value of 0.5 in deep water samples, when b was lowest. This must be interpreted cautiously since such clear water in nature is highly unlikely. Most likely, this resulted from significant error in the b calculation (c-a) at these low pigment concentrations.

Values of \tilde{b}_b were compared in this coccolithophore bloom as well as in chlorophyll-dominated waters (using the least squares relationship of Gordon and Morel 1983; their p. 62). Plots of $\tilde{b}_b 550$ vs $\tilde{b}_b 440$ showed the characteristic decrease of $\tilde{b}_b 550$ and $\tilde{b}_b 440$ in turbid water whether chlorophyll or calcite dominated the scattering (Fig. 11). In other words, backward scattering decreased relative to total scatter in the coccolithophore bloom for scattering values up to 3 m^{-1} (Fig. 7) or chlorophyll concentrations up to $10 \mu\text{g L}^{-1}$. At low chlorophyll concentrations with no suspended calcite, $\tilde{b}_b 440 > \tilde{b}_b 550$. When the chlorophyll a concentration exceeds 1 mg m^{-3} , $\tilde{b}_b 550 > \tilde{b}_b 440$; the volume scatter function is changing as a function of both chlorophyll and wavelength. In the coccolithophore bloom, $\tilde{b}_b 440$ always exceeded $\tilde{b}_b 550$ and the ratio $\tilde{b}_b 550 / \tilde{b}_b 440$ was essentially constant at high coccolith concentrations (Fig. 11). Thus, backscattering was a constant fraction of total scattering at the two wavelengths. For plots of $\tilde{b}_b 550$ vs $\tilde{b}_b 440$, the data for chlorophyll-dominated vs. calcite-dominated waters intersected at a chlorophyll concentration of about $0.25 \mu\text{g L}^{-1}$ and coccolith

concentration of about $100,000 \text{ mL}^{-1}$, implying similarly shaped volume scattering functions. Moreover, this confounding effect of variable chlorophyll made for a poor relationship between coccolith concentration and \tilde{b}_b in the coccolithophore bloom in the North Atlantic.

In previous coccolithophore blooms, coccolith concentration has been best calculated based on 550nm backscattering or reflectance, not \tilde{b}_b , because the former is less affected by chlorophyll a. Unfortunately, coccolith reflectance still contaminates the 440nm absorption band of chlorophyll (Gordon et al. 1988; Balch et al. 1991, Ackleson et al. 1994), which causes R_{440}/R_{550} to increase, and the calculated pigment concentration to be underestimated (Morel and Prieur 1977). The extent of this error still needs to be defined. To do this, one must first define the quantitative relationship between suspended calcite concentrations or coccolith concentrations, absorption, and scatter. This was done in this meso-scale coccolithophore patch in the north Atlantic and is the subject of Balch et al. (submitted).

The vertical distribution of calcite light scatter

Vertical profiles of light scatter in the mesoscale coccolithophore feature may have been influenced by several processes: sinking of plated cells and detached coccoliths, production and detachment of coccoliths at depth, grazing and defecation of coccoliths, and vertical mixing. While it is not possible to quantitatively determine the importance of these various processes using this data set, a discussion of the qualitative impact of these processes is in order, given the space and time constraints of the bloom.

To estimate the importance of sinking to our optical profiles, we needed to know the time scale of bloom formation. On June 10 at 20°W and 60°N , there was no high reflectance apparent in the satellite imagery, however, the bloom was well underway by 15 June (Holligan et al. 1993). Thus, assuming June 10th as the start date of the surface bloom means that bloom ages may be overestimated. Nevertheless, a reasonable time scale

for the development of the optical profiles shown in Figure 2A is about 14 d. The issue becomes whether sinking coccoliths could explain the variability in the shape of the light scatter profiles that we observed.

Sinking rate estimates of detached coccoliths are rare in the literature. Bramlette (1961) cited a sinking rate for detached coccoliths of about 5000m in 10 years (or $\sim 1.4 \text{ m d}^{-1}$) but gave no details on the calculation. This seems too fast given the empirical data of Honjo (1976), who measured sinking rates of detached *E. huxleyi* coccoliths at 0.14 m d^{-1} . To assess the applicability of Honjo's sinking rates to other species, classic stokes sinking rates were calculated for comparison. According to Eppley et al. (1967), based on earlier work of McNown and Malaika (1950), the sinking velocity can be described by the equation:

$$v_s = (\rho_c - \rho_w) V g / (3K \eta D \pi) \quad (3)$$

where v_s is the sinking rate (m s^{-1}), ρ_c and ρ_w are the density of the calcite (2700 kg m^{-3}) and water (1025 kg m^{-3}) respectively, V is the coccolith volume ($1.227 \times 10^{-18} \text{ m}^3$), g is the gravitational constant (9.8 m s^{-2}), K is a shape factor (which for flat discs at low Reynolds numbers $= 1.35$; see McNown and Malaika 1950; their fig. 4), η is the dynamic viscosity ($1.08 \times 10^{-3} \text{ Kg(ms)}^{-1}$ at 20°C), and D is the nominal diameter of an oval coccolith ($D = 1.156 \times 10^{-6} \text{ m}$ defined as $2(abc)^{0.333}$ where a , b , and c equal one-half of the thickness ($0.25 \mu\text{m}$), length ($2.8 \mu\text{m}$), and width ($2.2 \mu\text{m}$) respectively). The sinking rate calculated from the above equation was 0.11 m d^{-1} in good agreement with Honjo (1976). Thus the deepest that surface coccoliths could have sunk in 14 d was about 2m, so sinking of detached coccoliths would not have been expected to significantly influence the optical profiles over a fortnight.

The backscattering profile from 24 June 1991 (Figs. 2A and B) showed little calcite-dependent light scattering deeper than 40m depth. The mixed layer at this station

was about 11 m thick. Given the above sinking rates, it would have been impossible for detached coccoliths to sink from 11m to 40m in two weeks as this would have required a minimum net sinking velocity of about 2 m d^{-1} . It is possible that the coccoliths sank while attached to cells. Had the calcite been precipitated at 20m, and sunk to 40m attached to cells, then a 1.4 m d^{-1} sinking rate would have been required, close to Eppley et al.'s sinking rate for plated *E. huxleyi* cells (1.3 m d^{-1} ; Eppley et al. 1967). However, there are two important factors which should be kept in mind when discussing the optical impact of sinking plated cells: 1) coccolith-specific light scatter is generally thought to be greater when the coccoliths are *detached* from cells, not attached (Holligan et al. 1983). Thus, faster-sinking plated coccolithophore cells may alter the light scatter profile, but their optical impact is not as great as the slowly sinking detached coccoliths, 2) microscopic examination of water at 40m at the station given in Figure 2A revealed both detached and attached coccoliths. Fecal pellets also could have carried the coccoliths from the surface to 40m in less than a day (sinking rates $>150 \text{ m d}^{-1}$; see Honjo 1976) but the major impact of coccolith grazing is not moving coccoliths a few meters depth, but stripping coccoliths from the euphotic zone (Honjo 1976).

Physical overturn certainly could have mixed surface coccoliths downwards to achieve the optical profiles observed in Figure 2. However, had vertical mixing been involved in transferring coccoliths to depth, then the temperature profile also should have been isothermal to 40m, which was not the case (see temperature profile in Fig. 2B).

In situ calcification and coccolith detachment remains the most likely factor affecting the profile of light scatter shown in Figure 2. Fernandez et al. (1993) demonstrated active calcification at depth in the same part of the bloom that we sampled. Given their observed calcification rates (about $1 \text{ mg m}^{-3} \text{ d}^{-1}$ at 38m; see their figure 8D), and a carbon per coccolith of 0.25 pgC (Balch et al. 1991), then over 14d, the final coccolith concentrations should have been about $56 \times 10^3 \text{ coccoliths mL}^{-1}$. Furthermore, using the relationship between coccolith concentration and b_b' (Balch et al. 1991; their Fig. 11A & B), then

56,000 coccoliths mL^{-1} would have produced $b_b'_{440}$ and $b_b'_{550}$ of 1.09×10^{-2} and $8.24 \times 10^{-3} \text{ m}^{-1}$, respectively. This is within 25-30% of the values that we observed at 40m in Fig. 2A and 2B, reasonably close given the broad assumptions involved.

In summary, the subsurface scatter profiles probably resulted from at least two possible mechanisms: 1) plated, sinking coccolithophores shedding plates at depth (thus, the calcite originated from shallower depths) or 2) *in situ* calcification and deplating at depth by neutrally buoyant cells. Distinction between these two hypotheses will not only help elucidate the vertical distribution of calcite-dependent light scatter in the sea, but it will help in the interpretation of the complex ecology of these organisms. Moreover, the distinction is relevant to geochemical issues such as interpreting the calcite stable isotope signatures in the surface ocean, their extent of disequilibrium and resulting effect on the sedimentary isotope record (Paull and Balch 1994).

References

- Ackleson, S., W. M. Balch, P. M. Holligan. 1994. The response of water-leaving radiance to particulate calcite and pigment concentration: a model for Gulf of Maine coccolithophore blooms. *J. Geophys. Res.* **99**: 7483-7499.
- Aiken, J. and I. Bellan. 1990. Optical oceanography: An assessment of a towed method. p.39-57. *In* P. J. Herring, A. K. Campbell, M. Whitfield, and L. Maddock [eds.], *Light and life in the sea*. Cambridge University Press.
- Aiken, J. G. F. Moore and P. M. Holligan. 1992. Remote sensing of oceanic biology in relation to global climate change. *J. Phycol.* **28**: 579-590.
- Balch W. M., R. W. Eppley, M. R. Abbott and F. M. H. Reid. 1989. Bias in satellite-derived pigment measurements due to coccolithophores and dinoflagellates. *J. Plank. Res.* **11**: 575-581.
- Balch, W. M. , P. M. Holligan, S. G. Ackleson, and K. J. Voss. 1991. Biological and optical properties of mesoscale coccolithophore blooms in the Gulf of Maine. *Limnol. Oceanogr.* **36**: 629-643.
- Balch, W. M., P. M. Holligan and K. A. Kilpatrick. 1992. Calcification , photosynthesis and growth of the bloom-forming coccolithophore, *Emiliania huxleyi*. *Cont. Shelf Res.* **12**: 1353-1374.
- Balch, W. M. and K. A. Kilpatrick. 1992. Particulate reflectance measurements of phytoplankton. *J. Plank. Res.* **14**: 721-735.
- Balch, W.M., K.A. Kilpatrick, and P.M. Holligan. 1993. Coccolith formation and detachment by *Emiliania huxleyi* (Prymnesiophyceae). *J. Phycol.* **29**: 566-575.
- Balch, W. M., K. A. Kilpatrick, P. Holligan, D. Harbour, and E. Fernandez. The 1991 coccolithophore bloom in the central north Atlantic. II- Relating optics to coccolith concentration. *Limnology and Oceanography*. submitted.

- Beardsley, G. F. and J. R. V. Zaneveld. 1969. Theoretical dependence of the near-asymptotic apparent optical properties on the inherent optical properties of sea water. *J. Opt. Soc. Am.* 59: 373-377.
- Berge, G. 1962. Discoloration of the sea due to *Coccolithus huxleyi* "bloom". *Sarsia* 6: 27-40.
- Birkenes, E. and T. Braarud. 1952. Phytoplankton in the Oslo fjord during a "*Coccolithus huxleyi* summer". *Avhandl. Norske Videnskaps-Akad. Oslo, I. Mat. Naturv. Kl.* 2: 1-23.
- Braarud, T. 1945. A phytoplankton survey of the polluted waters of inner oslo fjord. *Hvalrad. Skr.* 28: 1-142.
- Braarud, T. 1963. Reproduction in the marine coccolithophorid *Coccolithus huxleyi* in culture. *Pubbl. staz. zool. Napoli.* 33: 110-116.
- Bramlette, M. N. 1961. Pelagic Sediments.p. 345-366. *In* M. Sears [ed.], *Oceanography*, ed. . Am. Assoc. for the Adv. of Science, Washington, D.C..
- Bricaud, A., J. R. V. Zaneveld and J. C. Kitchen. 1992. Backscattering efficiency of coccolithophorids: use of a three-layered sphere model. G. D. Gilbert [ed.], *Proceedings of the Society of Photo-Optical Instrumentation Engineers.- Ocean Optics IV.* 1750: 27-33.
- Brice, B. A., M. Halwer, and R. Speiser. 1950. Photoelectric light-scattering photometer for determining high molecular weights. *J. Opt. Soc. Amer.* 40: 768-778.
- Brongersma-Saunders, M. 1957. Mass mortality in the sea. *Geol. Soc. Am. Mem.* 67: 941-1010.
- Brown, C. and J. Yoder. 1993. Distribution pattern of coccolithophorid blooms in the Western North Atlantic. *Cont. Shelf Res.* 14:175-198.
- Brown, O. and H. Gordon. 1974. Size-refractive index distribution of clear coastal water particulates from light scattering. *Applied Optics* 13: 2874-2881.

- Eppley, R. W., R. W. Holmes and J. D. H. Strickland. 1967. Sinking rates of marine phytoplankton measured with a fluorometer. *J. exp. mar. Biol. Ecol.* **1**: 191-208.
- Fernandez, E., P. Boyd, P. M. Holligan and D. S. Harbour. 1993. Production of organic and inorganic carbon within a large scale coccolithophore bloom in the north Atlantic Ocean. *Mar. Ecol. Prog. Ser.* **97**: 271-285.
- Fukushima, H, and J. Ishizaka. 1993. Special features and applications of CZCS data in Asian waters, in press, *In "Ocean Colour: Theory and Applications in a Decade of CZCS Experience"*. Kluwer Academic, Boston, MA.
- Gordon, H. 1976. Radiative transfer in the ocean: A method for determination of absorption and scattering properties. *Appl. Opt.* **15**: 2611-2613.
- Gordon, H. and A. Y. Morel. 1983. Remote Assessment of Ocean Color for Interpretation of Satellite Visible Imagery- A Review. Springer-Verlag.
- Gordon, H. R., R. C. Smith, and J. R. V. Zaneveld. 1980. Introduction to Ocean Optics. in S. Duntley [ed.], *Proceedings of the Society of Photo-Optical Instrumentation Engineers.- Ocean Optics IV.* **208**: 14-55.
- Gordon, H. R., O. B. Brown, R. H. Evans, J. W. Brown, R. C. Smith, K. S. Baker, and D. K. Clark. 1988. A semianalytic radiance model of ocean color. *Journal of Geophysical Research* **93**: 10909-10924.
- Green, J. C., K. Perch-Nielsen and P. Westbroek. 1990. Prymnesiophyta, p. 293-317. *In* L. Margulis, J.O. Corliss, M. Melkonian and D.J. Chapman [eds.] *Handbook of Protoctista*, Jones and Bartlett, Boston, MA.
- Groom, S., and P. M. Holligan. 1987. Remote sensing of coccolithophore blooms. *Adv. Space Res.* **7**: 73-78.
- Halldal, P. 1953. Phytoplankton investigations from Weather Ship M in the Norwegian Sea, 1948-49. Including observations during the "Armauer Hansen" cruise July 1949. *Hvalradets Skrifter Norske Videnskaps-Akad. Oslo* **38**: 3-91.

- Hentschel, E. 1936. Allgemeine Biologie des Sudatlantischen Ozeans. Wiss. Ergeb. deut. Exped. "Meteor" **11**: 1-344.
- Hodkinson, J. R. and J. I. Greenleaves. 1963. Computations of light-scattering and extinction by spheres according to diffraction and geometrical optics and some comparisons with the Mie theory. J. Opt. Soc. Amer., **53**: 577-588.
- Holligan, P. M. , M. Viollier, D. S. Harbout, P. Camus, and M. Champagne-Philippe. 1983. Satellite and ship studies of coccolithophore production along a continental shelf edge. Nature **304**: 339-342.
- Holligan, P. M., E. Fernandez, J. Aiken, W. M. Balch, P. Boyd, P. H. Burkill, M. Finch, S. B. Groom, G. Malin, K. Muller, D. A. Purdie, C. Robinson, C. Trees, S. Turner, and P. van der Wal. 1993. A biogeochemical study of the coccolithophore, *Emiliana huxleyi*, in the north Atlantic. Global Bio. Cycles **7**: 879-900.
- Holm-Hansen, O., C. J. Lorenzen, R. W. Holmes, and J. D. H. Strickland. 1965. Fluorometric determination of chlorophyll. J. Cons. Perm. Int. Explor. Mer. **30**: 3-15.
- Honjo, S. 1976. Coccoliths: production, transportation and sedimentation. Marine Micropaleontology. **1**: 65-79.
- Jerlov, N. G. 1976. Marine Optics. Elsevier.
- Kirk, J. T. O. 1994. Light & Photosynthesis in Aquatic Ecosystems, 2nd ed. Cambridge University Press.
- Kitchen, J. and R. Zaneveld. 1990. On the noncorrelation of the vertical structure of light scattering and chlorophyll a in case I waters. Journal Geophys. Res. **95**: 20237-20246.
- Kortüm, G. 1969. Reflectance Spectroscopy. Springer-Verlag, 336 p.
- Kubelka, P. and Munk, F. 1931. Ein beitrag zur optik der farbanstriche. Z. Tech. Phys. **12**: 593-601.

- Lapota, D., C. Galt, J. R. Losee, and D. Howard. 1988. Observations and measurements of planktonic bioluminescence in and around a milky sea. *J. Exp. Mar. Biol. Ecol.* **119**: 55-81.
- Lohmann, H. 1920. Die Coccolithophoridae, eine Monographie der Coccolithenbildenden Flagellaten. *Arch. Protistenk.* **1**: 89-165.
- McNown, J. S. and J. Malaika. 1950. Effects of particle shape on settling velocity at low Reynolds numbers. *Trans. Am. Geophys. Union.* **31**: 74-82.
- Mie, G. 1908. Beitrage zur Optik truber Medien, speziell kolloidalen Metall-losungen. *Ann. Phys.*, **25**: 377.
- Milliman, J. 1993. Production and accumulation of calcium carbonate in the ocean: budget of a nonsteady state. *Global Biogeochemical Cycles.* **7**: 927-957.
- Mitchell, B. G. 1990. Algorithms for determining the absorption coefficient of aquatic particulates using quantitative filter techniques (QFT). *SPIE Ocean Optics X*, **1302**, 137-147.
- Mitchell, B. G. and D. A. Kiefer. 1988. Chlorophyll a specific absorption and fluorescence excitation spectra for light-limited phytoplankton. *Deep-Sea Res.* **35**: 639-663.
- Morel, A. 1987. Chlorophyll-specific scattering coefficient of phytoplankton, a simplified theoretical approach. *Deep Sea Res.* **34**: 1093-1105.
- Morel, A. and Y.-H. Ahn. 1991. Optics of heterotrophic nanoflagellates and ciliates: A tentative assessment of their scattering role in oceanic waters compared to those of bacterial and algal cells. *J. Mar. Res.* **49**: 177-202.
- Morel, A. and A. Bricaud. 1981. Theoretical results concerning light absorption in a discrete medium, and application to specific absorption of phytoplankton. *Deep Sea Res.* **28**: 1375-1393.
- Morel, A. and L. Prieur. 1977. Analysis of variations in ocean color. *Limnol. Oceanogr.* **22**: 709-722.

- Paasche, E. 1962. Coccolith formation. *Nature* **193**: 1094-1095.
- Pak, H. 1970. The Columbia River as a source of marine light scattering particles. Ph.D. Dissertation. Oregon State University, 110 pp.
- Paull, C. K. and W. M. Balch. 1994. Oxygen isotopic disequilibrium in coccolith carbonate from phytoplankton blooms. *Deep-Sea Res.* **41**: 223-228.
- Petzold, T. J. 1972. Volume scattering functions for selected ocean waters. Univ. Calif. Scripps Inst. Oceanogr. Tech. Rep. 72-78.
- Petzold, T. J. and R. W. Austin. 1968. An underwater transmissometer for ocean survey work. *Underwater Photo-optical Instrument Applications. SPIE* **12**: 133-137.
- Smith, R. C. and K. S. Baker. 1981. Optical properties of the clearest natural waters (200-800 nm). *Applied Optics.* **20**: 177-184.
- Spilhaus, A. F. Jr. 1965. Observations of light scattering in sea water. Ph.D. dissertation. Massachusetts Institute of Technology, 168 pp.
- Trees, C. C., J. Aiken, H.-J. Hirche, and S. B. Groom. 1992. Bio-optical variability across the Arctic Front. *Polar. Biol.* **12**: 4554-4561.
- Voss, K. 1992. A spectral model of the beam attenuation coefficient in the ocean and coastal areas. *Limnol. Oceanogr.* **37**: 501-509.
- Voss, K. and R. W. Austin. 1993. Beam-attenuation measurement error due to small-angle scattering acceptance. *Am. Met. Soc.* **10**: 113-121.
- Westbroek, P., C. W. Brown, J. van Bleijswijk, C. Brownlee, G. Brummer, M. Conte, J. Egge, E. Fernandez, R. Jordan, M. Knappertsbusch, J. Stefels, M. Veldhuis, P. van der Wal, and J. Young. 1993. A model system approach to biological climate forcing. The example of *Emiliana huxleyi*. *Global and Planetary Change.* **8**: 27-46.
- Yentsch, C. S. and D. W. Menzel. 1963. A method for the determination of phytoplankton chlorophyll and phaeophytin by fluorescence. *Deep-Sea Res.* **10**: 221-231.

Yentsch, C. S. and D. A. Phinney. 1989. A bridge between ocean optics and microbial ecology. *Limnol. Oceanogr.* 34: 1694-1705.

Table 1- Dates (month.day), times (local) and positions (decimal degrees) of hydro-stations visited during t

DATE	time	JDAY	lat	lon
1991	(local)		<u>°N</u>	<u>°W</u>
6.17	2.50	168.10	55.84	19.94
6.17	12.08	168.50	56.01	19.99
6.18	9.50	169.40	58.18	20.01
6.19	1.00	170.04	60.00	20.00
6.19	12.00	170.50	60.00	20.00
6.19	21.20	170.88	59.99	19.84
6.19	21.33	170.89	60.03	19.99
6.20	15.42	171.64	61.67	19.95
6.21	19.50	172.81	62.99	20.00
6.21	19.50	172.81	63.56	21.33
6.22	9.50	173.40	61.52	22.60
6.23	1.17	174.05	61.08	22.70
6.23	11.00	174.46	61.11	22.71
6.24	1.00	175.04	61.10	22.71
6.24	18.75	175.78	61.12	23.02
6.26	9.50	177.40	59.65	20.97
6.26	9.50	177.40	59.64	21.10
6.27	15.83	178.66	61.18	15.18
6.28	0.50	179.02	61.20	15.16
6.29	3.75	180.16	61.14	14.81
6.29	14.33	180.60	60.95	15.55
6.30	16.12	181.67	61.02	14.71
7.01	17.50	182.73	57.35	12.67
7.02	10.10	183.42	56.39	8.61

Table 2- List of symbols, with definitions and units . Values are given when applicable.

a_p	phytoplankton absorption coefficient (m^{-1})
a_p^*	phytoplankton-specific absorption (m^{-2} (mg chl $^{-1}$))
b	Scattering coefficient (m^{-1})
b_b	Backscatter coefficient (m^{-1})
b_b'	Backscatter coefficient of calcite (m^{-1})
\bar{b}_b	Ratio of scatter to backscatter, also known as backscattering probability
β_θ	Volume scatter at angle θ (m^{-1} sr $^{-1}$)
c_{vls}	beam transmittance as measured with the Vis Lab Spectral Transmissometer (m^{-1})
c_{st}	beam transmittance as measured with a Sea Tech 0.25m pathlength transmissometer (m^{-1})
c_w	beam transmittance of water (m^{-1} ; value used here from Gordon et al. (1980)
D	nominal diameter of an oval coccolith ($1.156 \times 10^{-6}m$)
g	gravitational constant ($9.8m\ s^{-2}$)
η	dynamic viscosity ($1.08 \times 10^{-3}\ Kg(ms)^{-1}$ at 20°C)
K	shape factor (unitless; for flat discs at low Reynolds numbers =1.35)
Q	ratio of upwelling radiance to the upwelling irradiance toward zenith (unitless)
R	irradiance reflectance (defined as upward irradiance/downward irradiance)
ρ_c	density of the calcite ($2700\ kg\ m^{-3}$)
ρ_s	density of water ($1025\ kg\ m^{-3}$)
V	coccolith volume ($1.227 \times 10^{-18}\ m^3$)

Table 3. Statistical summary of linear optical relationships during the BOFS cruise. Table provides the name of the independent variable (Ind. Var.), Dependent variable (Dep. Var.), number of points, least-squares fit slope, standard error (s.e.) of the slope, least-squares fit intercept (Int), standard error of the intercept, coefficient of correlation, F statistic (equal to the regression mean square/residual mean square), and P, the probability that the slope is equal to 0 (* indicates $P < 0.001$, Type 1 error). Where regressions were performed using log transformed variables, this is shown in the first two columns.

Ind Var	Dep Var	n	Slope	s.e.	Int	s.e	r^2	F	P
Ln $b_b(440)$	Ln $\beta_0(440)$	157	4.913	1.68E-2	2.71E-3	7.77E-5	0.998	85058	*
Ln $b_b(550)$	Ln $\beta_0(550)$	156	3.891	1.65E-2	3.37E-3	7.07E-5	0.997	55573	*
$b_b(550)$	$b_b(440)$	156	0.762	7.99E-3	3.10E-4	1.98E-4	0.983	9124	*
$b_b'(550)$	$b_b'(440)$	154	0.766	9.06E-3	1.18E-5	1.68E-4	0.979	7148	*
ap(440)	chl <u>a</u>	253	0.0685	2.69E-3	2.91E-2	2.96E-3	0.721	648	*
ap(550)	chl <u>a</u>	253	0.0129	7.78E-4	8.15E-3	8.55E-4	0.521	273	*

Table 4- Best-fit parameters for empirical algorithm predicting $b(\lambda; \text{m}^{-1})$ from $bb(\lambda; \text{m}^{-1})$ in North Atlantic coccolithophore bloom.

λ (nm)	$b_{\text{max}}(\lambda)$	$bb_0(\lambda)$	$Kb(\lambda)$	r^2
440	4.44	4.41×10^{-3}	3.30×10^{-2}	0.84
550	3.64	4.02×10^{-3}	1.96×10^{-2}	0.86

Table 5- Data for solar zenith angle and the ratio of upwelling radiance to the upwelling irradiance toward zenith (Q) at 441 and 550nm. See text for details of measurements.

Lat (°N)	Lon (°W)	Date 1991	Time local	Stn no.	Zenith Sun Angle	Q441	Q550
59.983	19.948	19 Jun	1011	3	49.07	6.40	3.45
60.012	19.840	19 Jun	1215	4	38.33	5.98	5.98
60.030	19.817	19 Jun	1457	5	40.32	5.98	6.63
61.660	19.970	20 Jun	1400	7	38.8	4.54	5.039
63.207	21.608	21 Jun	1440	8	41.56	5.04	6.19
63.583	21.330	21 Jun	1821	9	61.85	6.19	7.60
61.517	22.598	22 Jun	0953	10	53.33	5.04	5.58
60.855	22.667	22 Jun	19.03	11	66.14	6.19	7.099
61.112	22.700	23 Jun	1058	12	45.98	5.40	5.40
61.112	22.738	23 Jun	1303	13	38.01	5.04	5.40
61.392	22.917	24 Jun	0950	14	53.48	5.21	5.21
60.917	22.900	24 Jun	1511	15	41.05	6.19	5.98
59.662	22.982	26 Jun	1043	17	46.92	6.41	6.86
59.623	21.082	26 Jun	1220	18	38.09	6.41	6.57
61.213	15.188	27 Jun	1534	19	45.78	8.14	7.10
61.158	15.230	28 Jun	0920	20	53.51	6.66	7.10
61.160	15.235	28 Jun	1216	22	37.71	6.41	6.41
61.172	15.205	28 Jun	1229	23	38.32	6.41	6.19
61.005	14.728	30 Jun	1454	26	38.82	6.41	6.41
Average						6.00	6.12

Figure Legend

Fig.1-Cruise track of the RRV Charles Darwin (cruise CD60) showing dates along the cruise track. MLML refers to the "Marine Light in the Mixed Layer" optical mooring at 59° 39' N x 20° 59' W.

Fig. 2- Vertical profiles of backscatter (bb) at two stations: A) 61° 07.03' N x 23° 01.4' W, 24 June 1991, 1845h local time; data for bb at 436nm B) same station as panel (A) except data are for bb at 546nm, C) 59° 39.1' N x 20° 58.4' W, 26 June 1991, 0930h local time; data for bb at 436nm D) same station as panel (C) except data are for bb at 546nm. Note change in scales for X and Y axes between panels A and B versus C and D.

Fig. 3- Map of the study area showing surface contours of A) particulate absorption coefficient at 440nm, ap_{440} ($\times 10^{-2} \text{ m}^{-1}$), B) particulate absorption coefficient at 550nm, ap_{550} ($\times 10^{-3} \text{ m}^{-1}$), C) backscattering coefficient at 440nm, bb_{440} ($\times 10^{-3} \text{ m}^{-1}$), D) backscattering coefficient at 550nm, bb_{550} ($\times 10^{-3} \text{ m}^{-1}$), E) calcite-specific backscattering coefficient at 440nm, bb'_{440} ($\times 10^{-3} \text{ m}^{-1}$), and F) calcite-specific backscattering coefficient at 550nm, bb'_{550} ($\times 10^{-3} \text{ m}^{-1}$). Station locations are shown with *'s.

Fig. 4- Vertical section along 20°W for A) ap_{440} ($\times 10^{-2} \text{ m}^{-1}$), B) ap_{550} ($\times 10^{-3} \text{ m}^{-1}$), C) bb_{440} ($\times 10^{-3} \text{ m}^{-1}$), D) bb_{550} ($\times 10^{-3} \text{ m}^{-1}$), E) bb'_{440} ($\times 10^{-3} \text{ m}^{-1}$), and F) bb'_{550} ($\times 10^{-3} \text{ m}^{-1}$). Sample locations and depths are shown with *'s.

Fig. 5- A) Raw uncorrected beam attenuation values for two transmissometers, the VLST and Sea Tech at 8 stations where both instruments were running simultaneously. Beam attenuation of water (cw) has been subtracted from each data set. The equation relating the raw data from the two instruments was: $cvl_{535}[0.108] = (1.05[0.072] \times cst_{660}) +$

0.207[0.071] ; $r^2 = 0.97$; $n=8$). Standard error of the dependent variable, slope and intercept are given in the square brackets. B) Same beam attenuation data as in (A) except data have been wavelength corrected to 550nm using the model of Voss (1992). The equation relating the wavelength-corrected results from the two instruments was: $cvlst_{550}[0.112] = (0.992[0.068] \times cst_{550}) + 0.215[0.074]$; $r^2 = 0.97$; $n=8$). C) Same beam attenuation data as in (B) except data have been wavelength corrected for differences in optical geometry according to Voss and Austin (1993). The equation relating the wavelength-corrected results from the two instruments was: $cvlst_{550}[0.130] = (0.910[0.062] \times cst_{550}) + 0.236[0.090]$; $r^2 = 0.97$; $n=8$).

Fig. 6- Total light scatter, b , versus total backscatter, b_{btot} ; A)440nm results, B)550nm results. Values of b were calculated as the difference between beam attenuation (corrected for wavelength and instrument geometry), and the sum of particulate absorption and water absorption. Values of b_b were calculated entirely independantly using volume scatter data from the Brice Phoenix Light Scattering photometer according to Gordon(1976). Least square fits are given in the text.

Fig. 7- Same data as in Fig. 6 except \tilde{b}_b is shown vs b_{tot} for A)440nm and B) 550nm.

Fig. 8- Advanced Very High Resolution Radiometer (AVHRR) image of 1991 coccolithophore bloom in the NE Atlantic Ocean. Image is from the corrected visible (channel 1) image of 19 June 1991. Regions of high reflectance appear as light areas in the image. Clouds and land were masked in each image and are black. This image was taken from NOAA 11 using the early afternoon pass for channel 1 and processed according to Groom and Holligan (1987). White contours show the same data as in figure 3f, superimposed on the image. The ship's location at the time of the image was $59^{\circ} 58.9' N$ x $19^{\circ} 59.5' W$.

Fig. 9- Maps of surface reflectance calculated as described in the text. A) 440nm reflectance (%) and B) 550nm reflectance (%).

Fig. 10- Comparison of predicted irradiance reflectance and measured irradiance reflectance at seven stations. A 1:1 line is shown for reference.

A) Data at 440nm. Least squares fit to these data is:

$$\text{Predicted } R_{440}[0.034] = 0.91[0.14] * \text{Measured } R_{440} - 0.012[0.027]; r^2 = 0.89; n = 7$$

B) Data at 550nm. Least squares fit to these data is:

$$\text{Predicted } R_{550}[0.023] = 0.83[0.10] * \text{Measured } R_{550} + 0.0086[0.018]; r^2 = 0.93$$

Standard errors of the slope, intercept, and predicted value are given in square brackets for both equations.

Fig. 11- $\tilde{b}_b 550$ vs $\tilde{b}_b 440$ for bloom calculated from bbtot and btot measurements (+ symbols). Variability of $\tilde{b}_b 550$ vs $\tilde{b}_b 440$ due to changes in chlorophyll concentration are shown for comparison (relationships given by Gordon and Morel, 1983); the two endpoint chlorophyll concentrations are shown for reference. A 1:1 line is also shown.

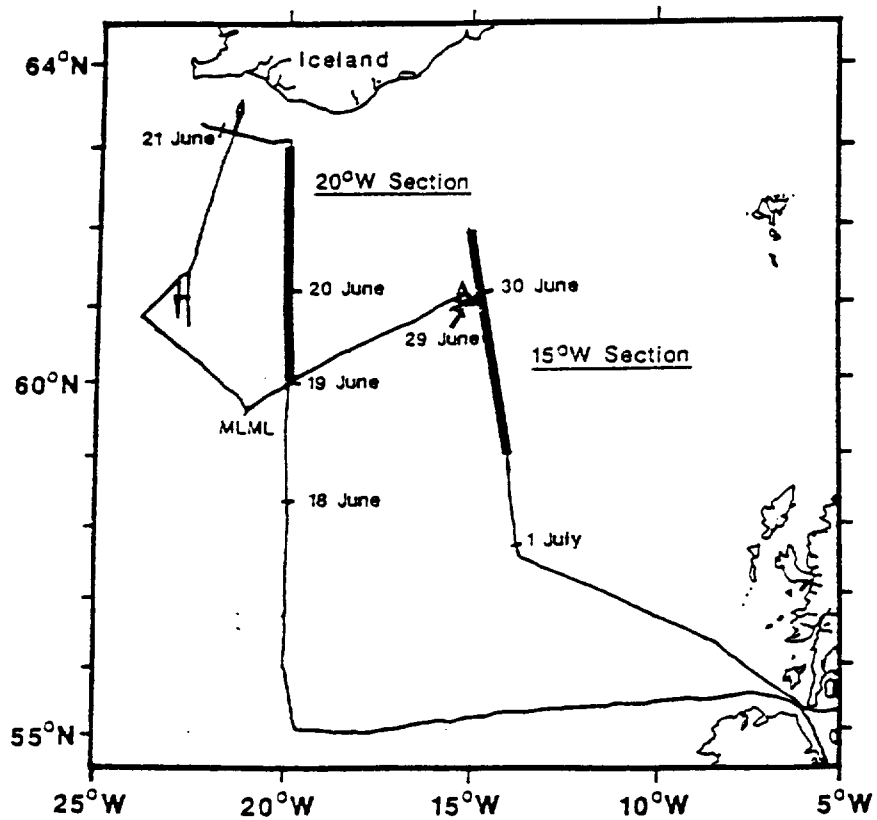
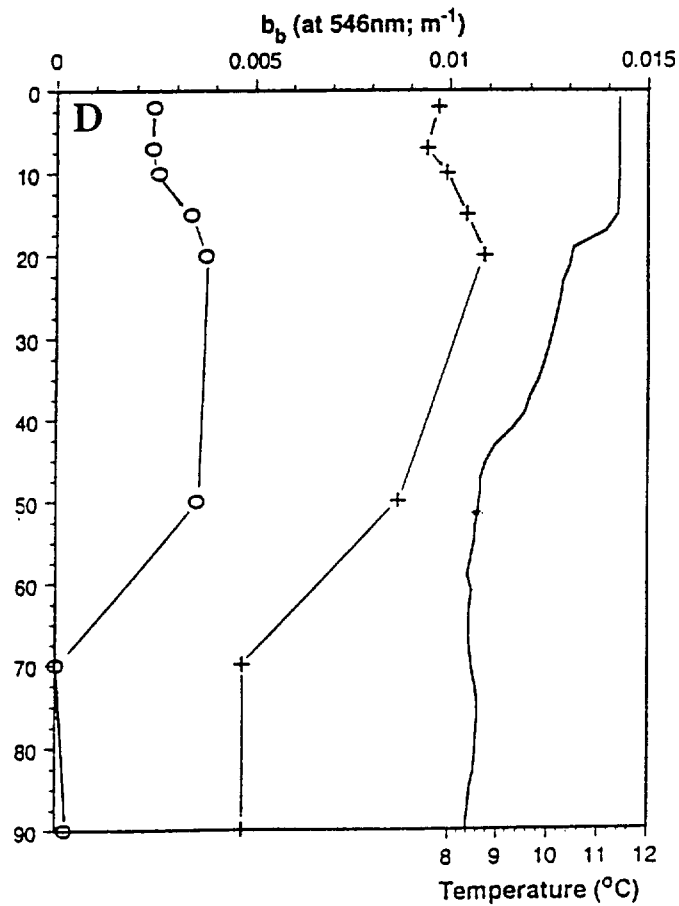
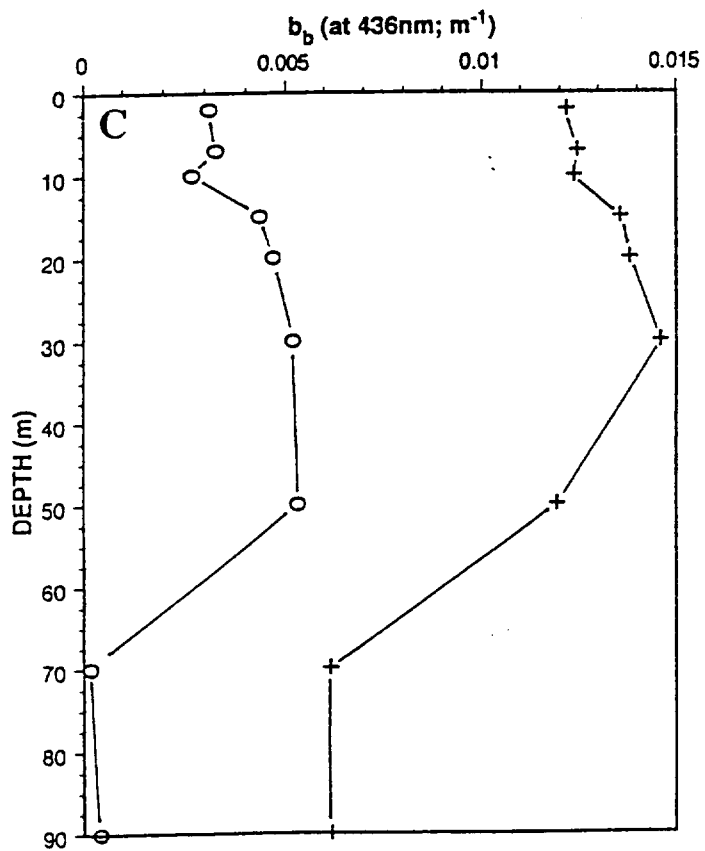
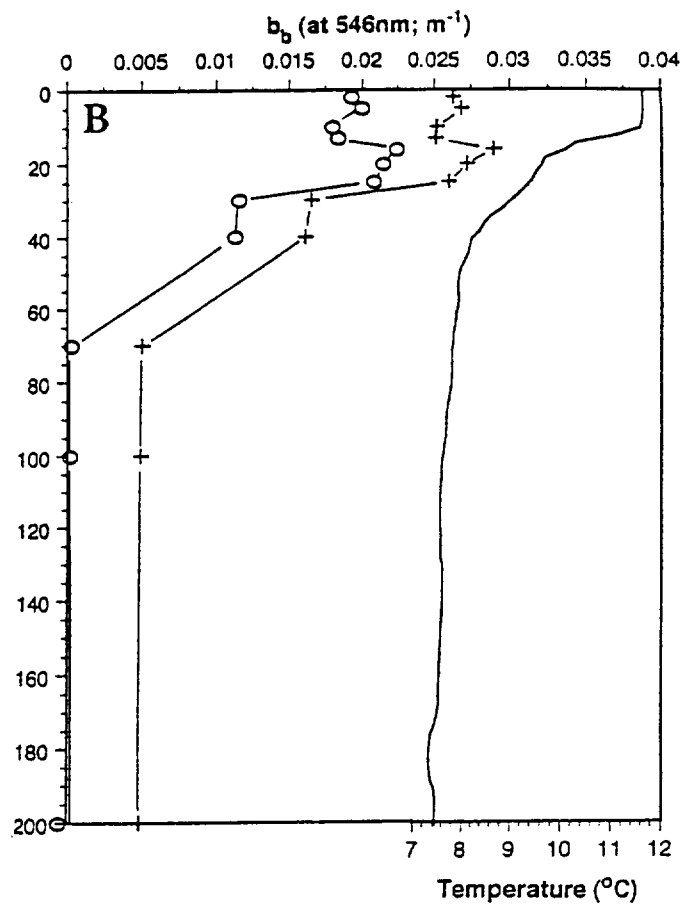
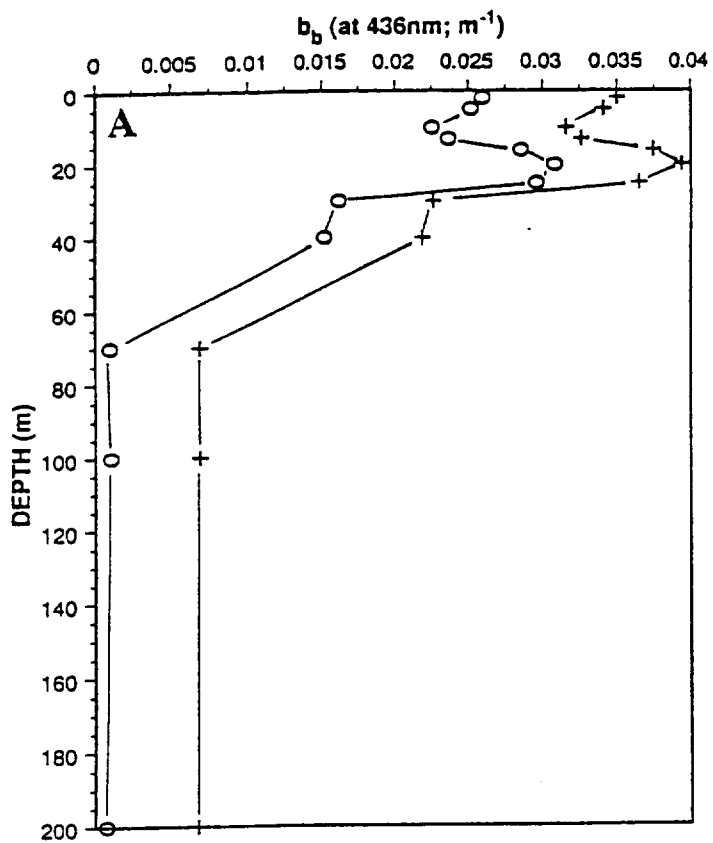
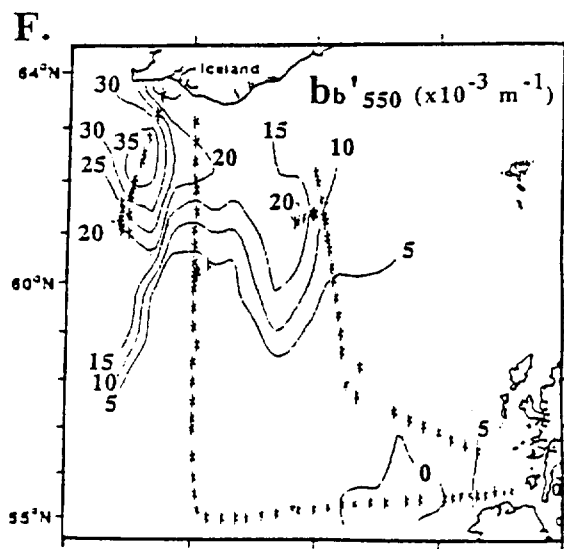
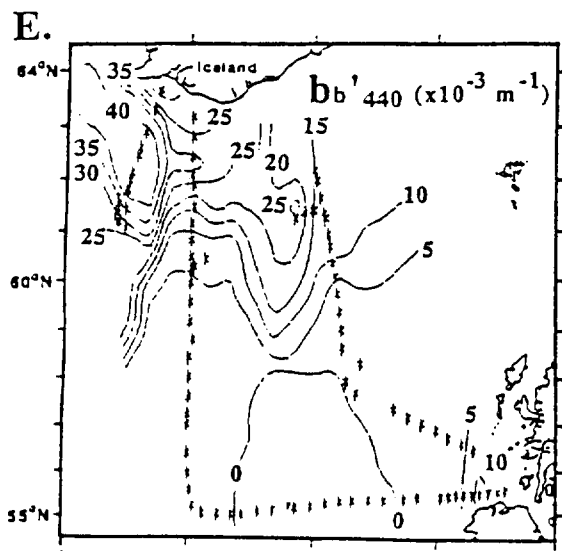
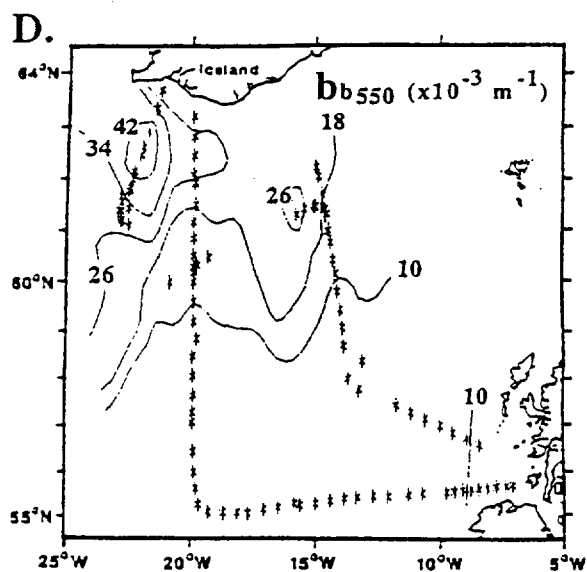
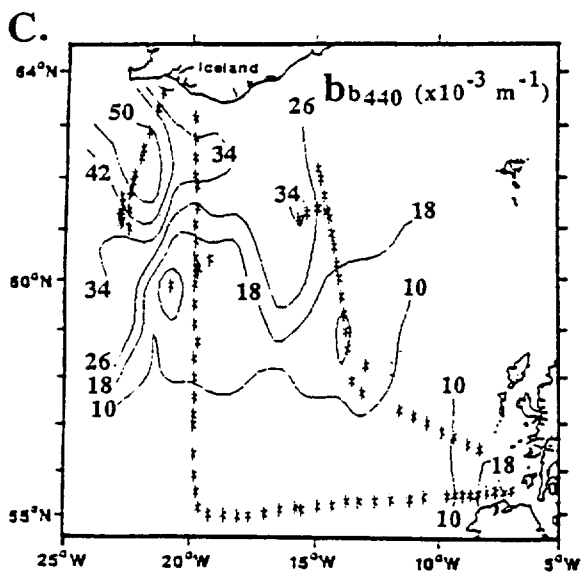
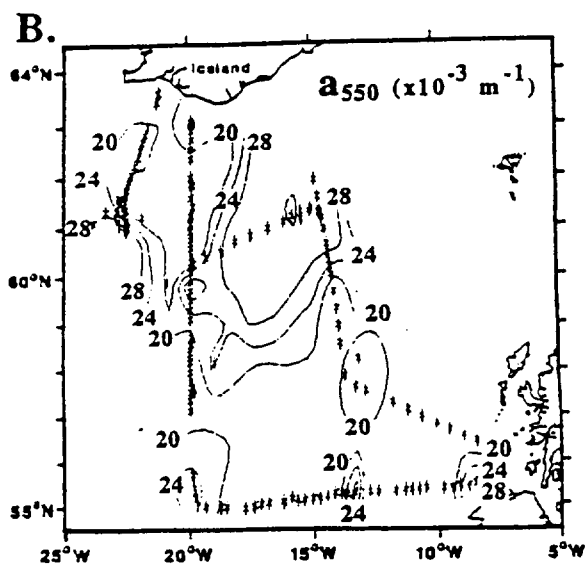
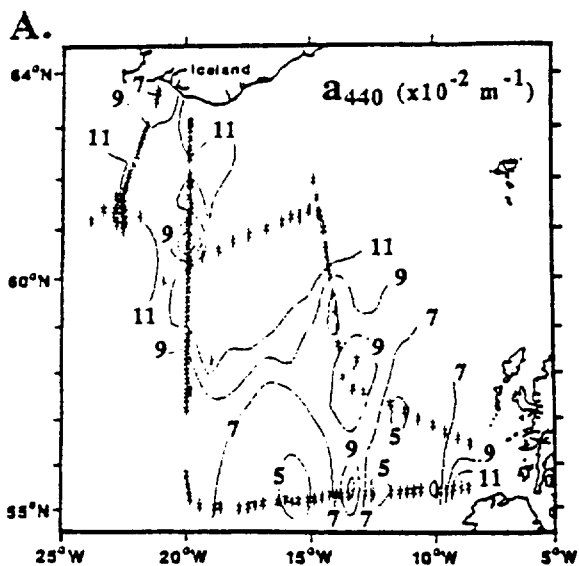
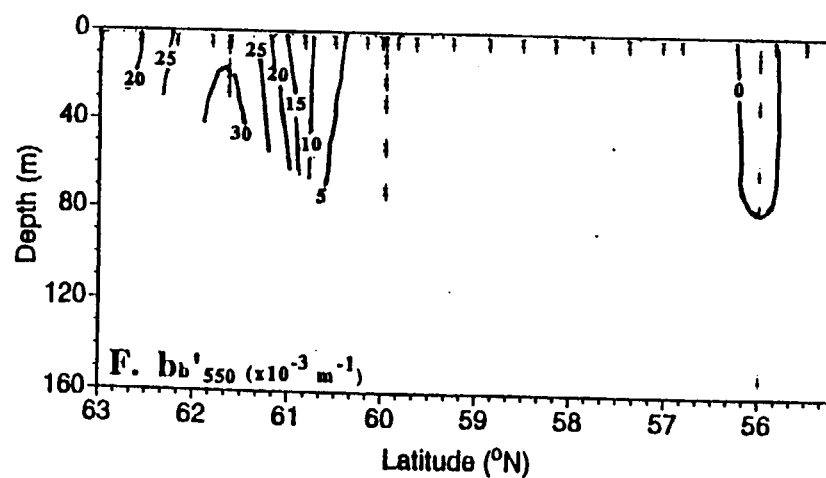
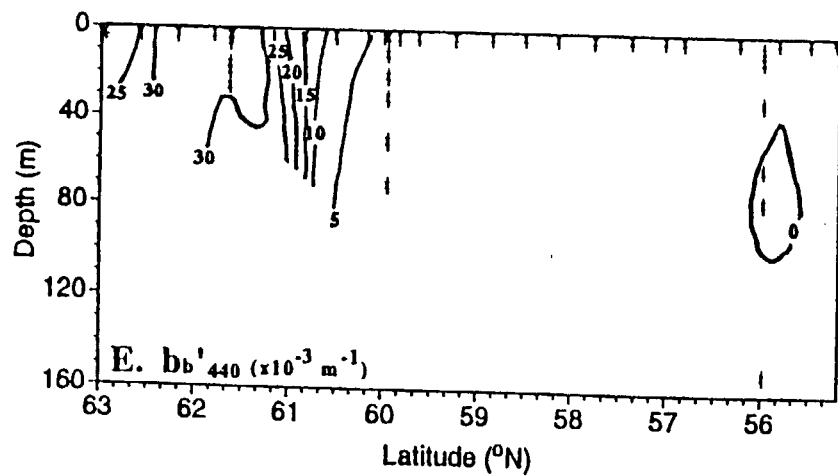
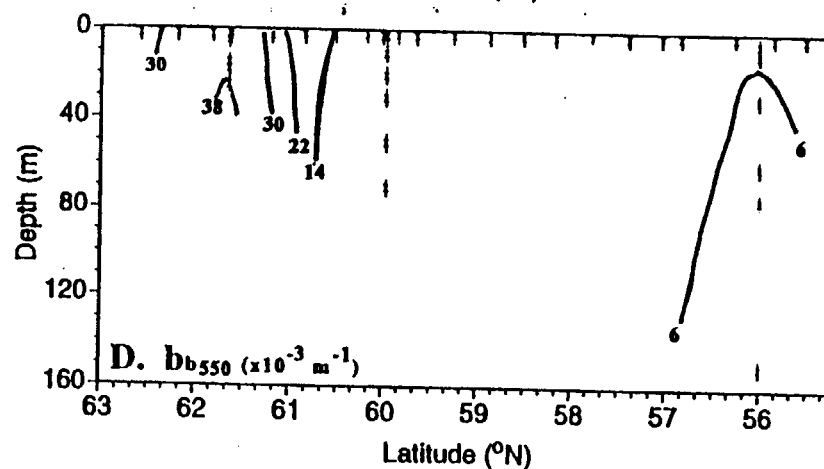
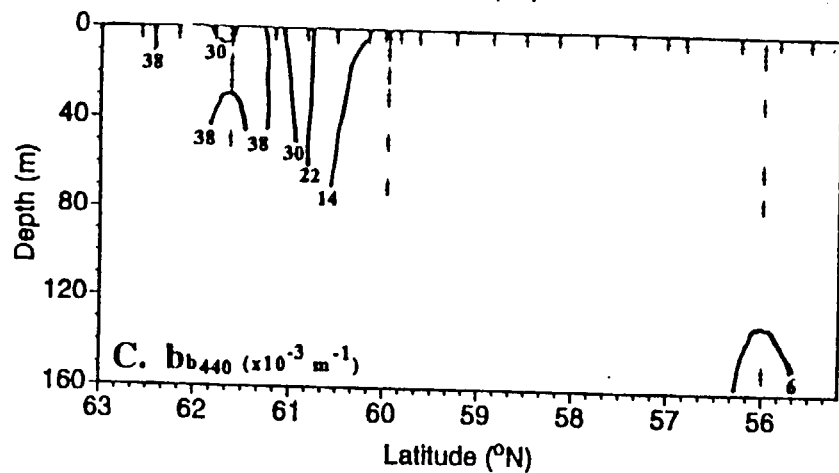
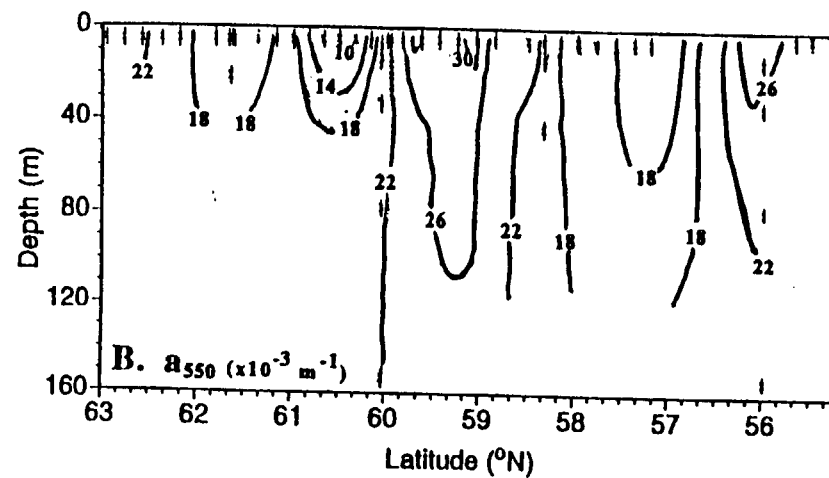
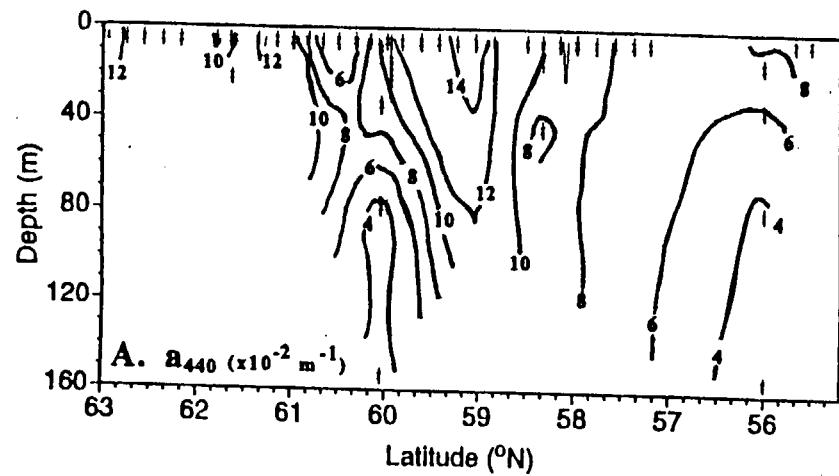
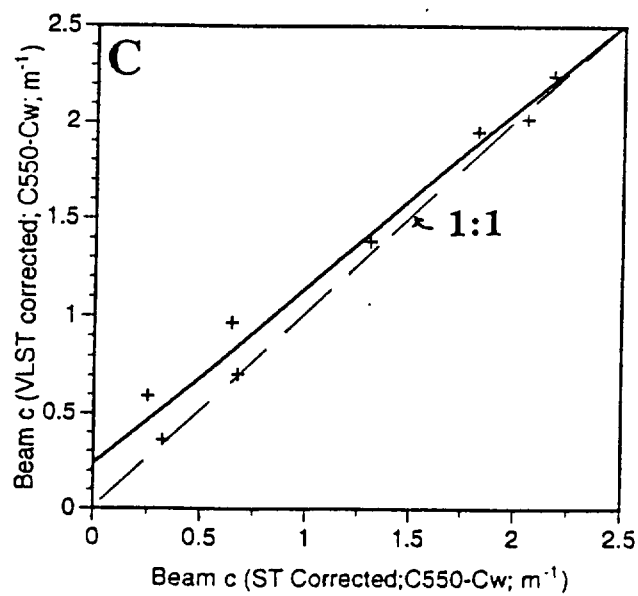
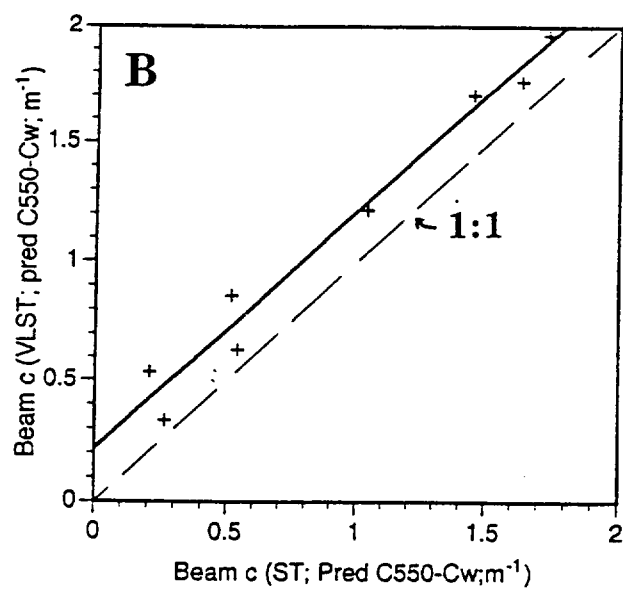
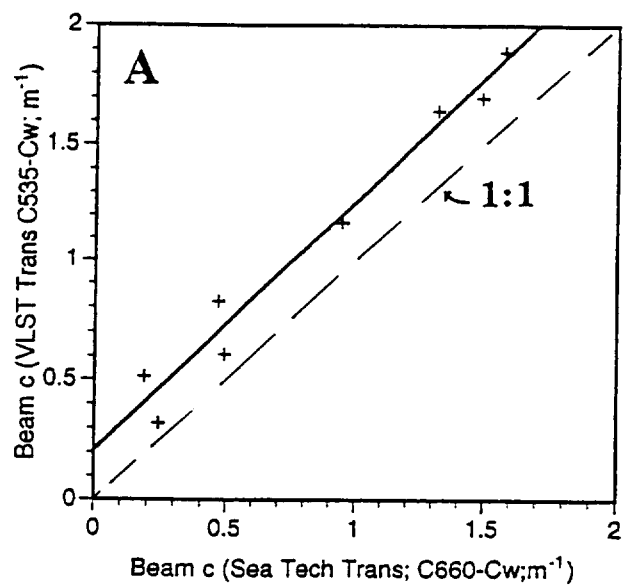


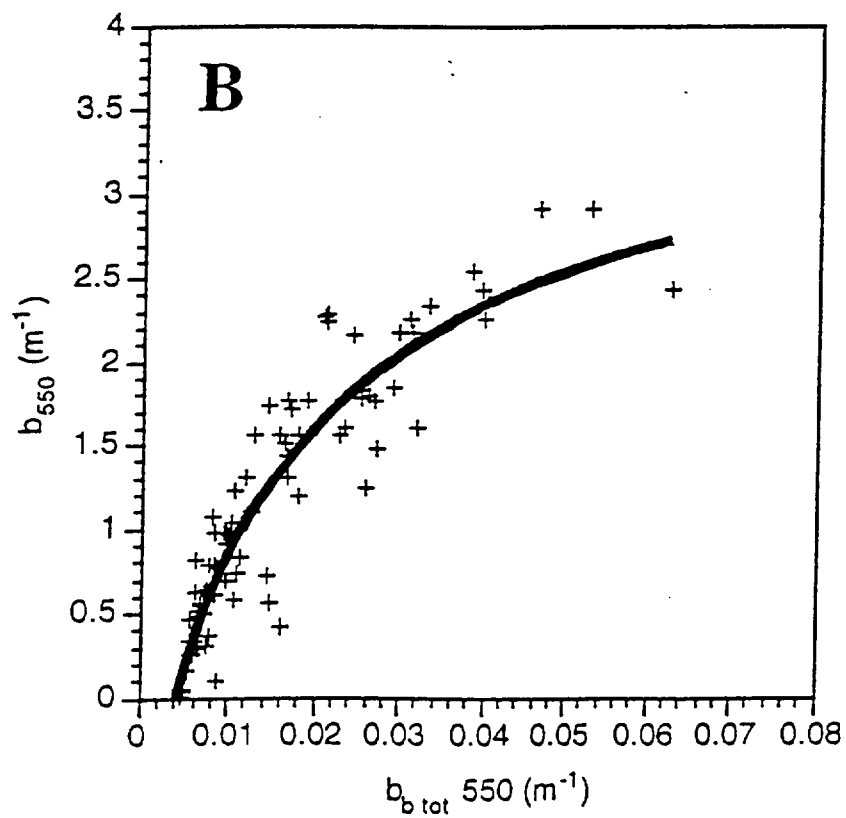
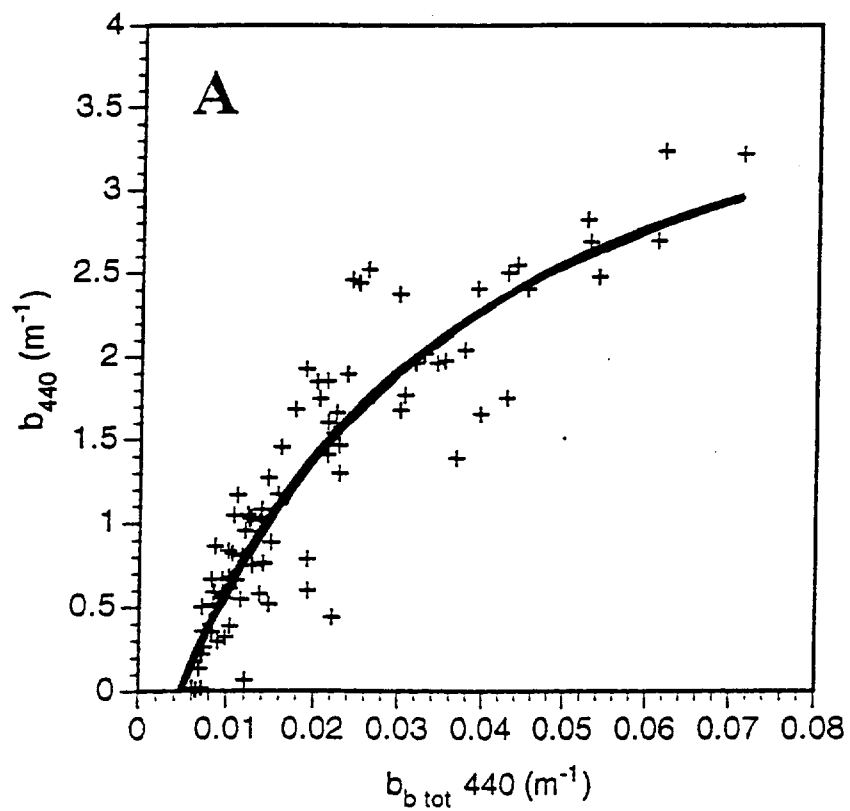
FIG 1

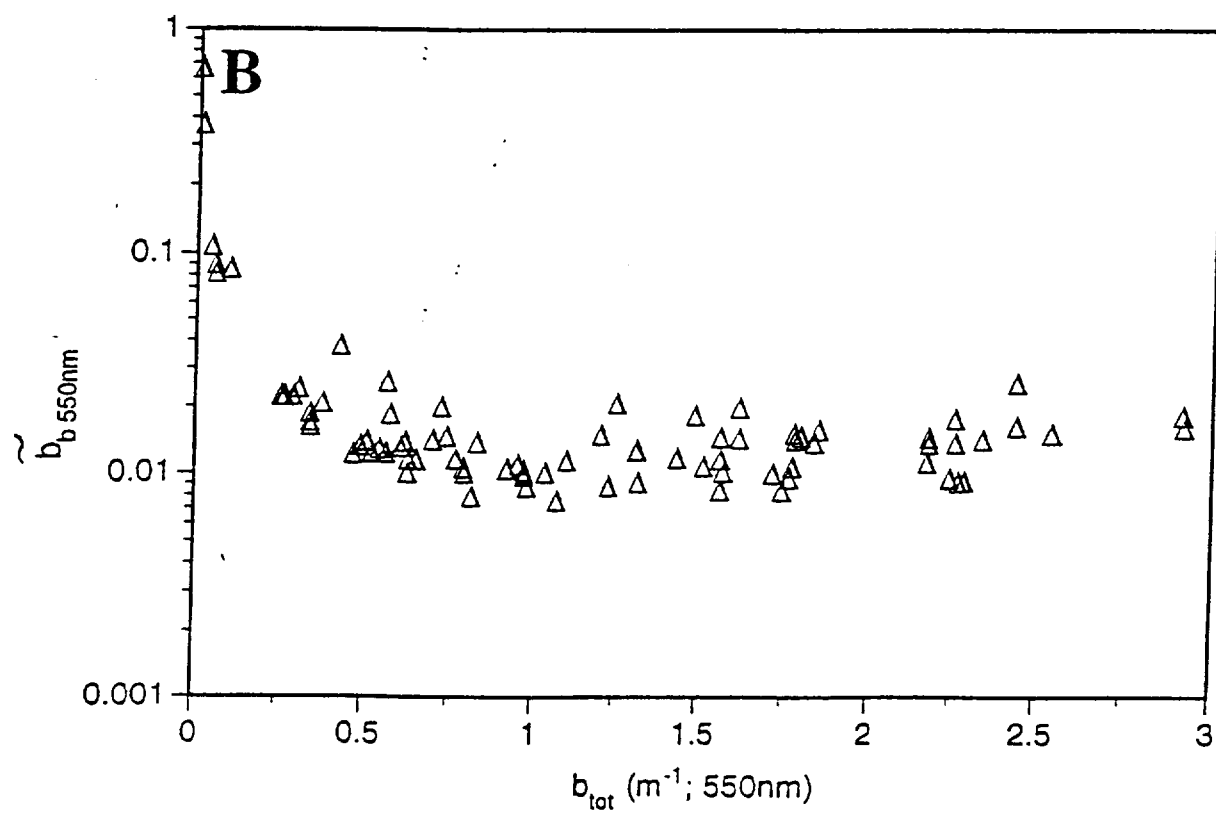
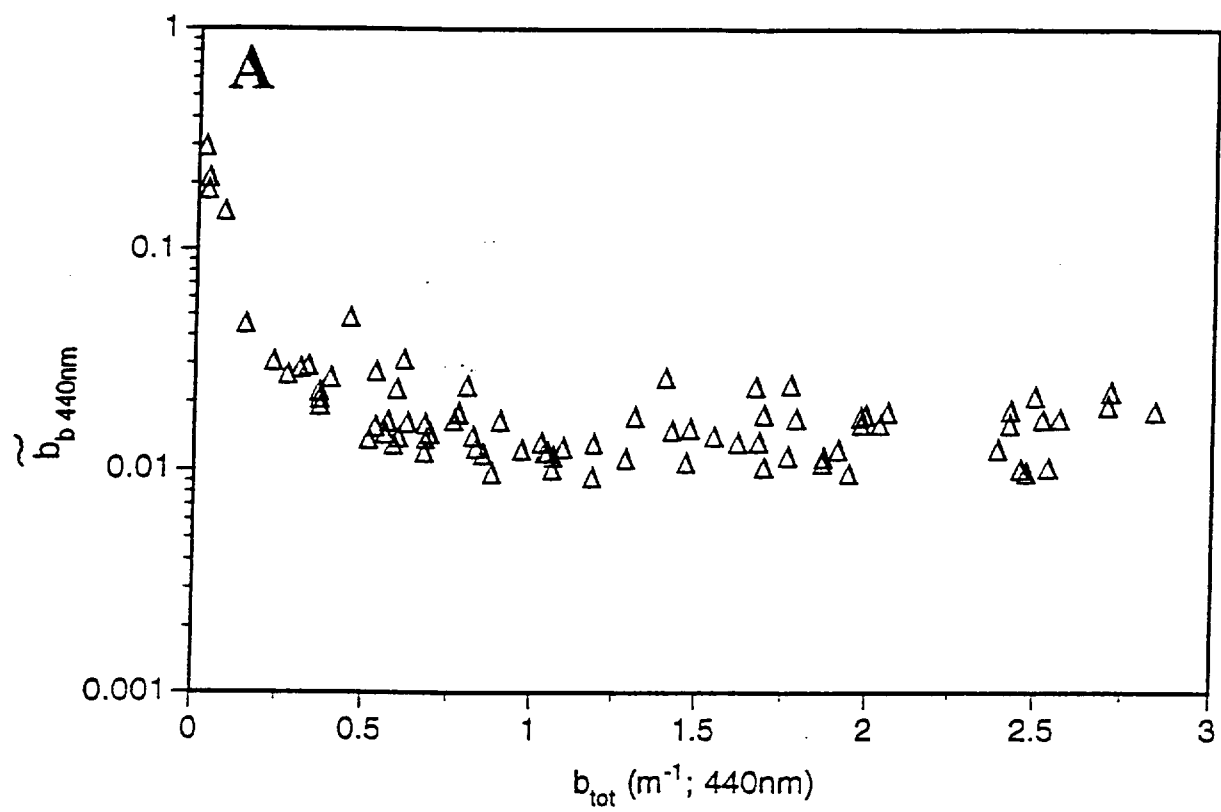


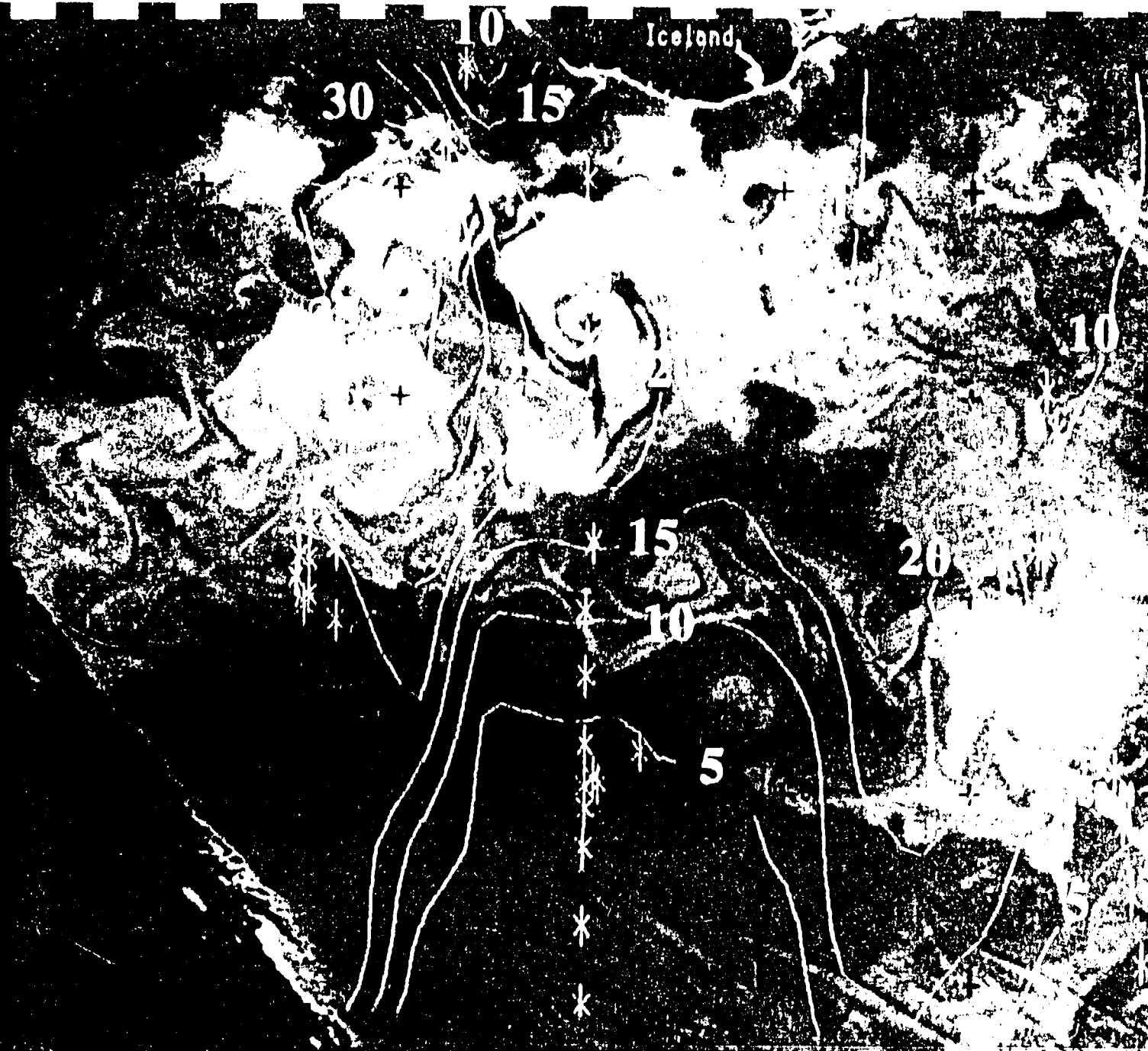




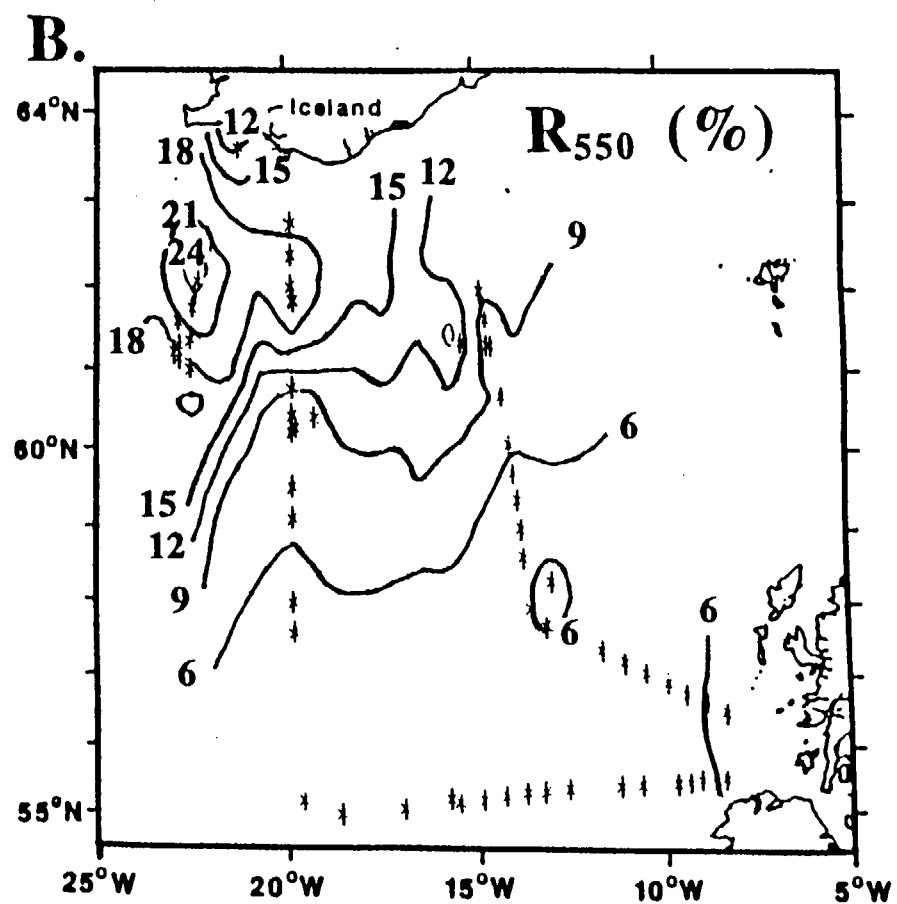
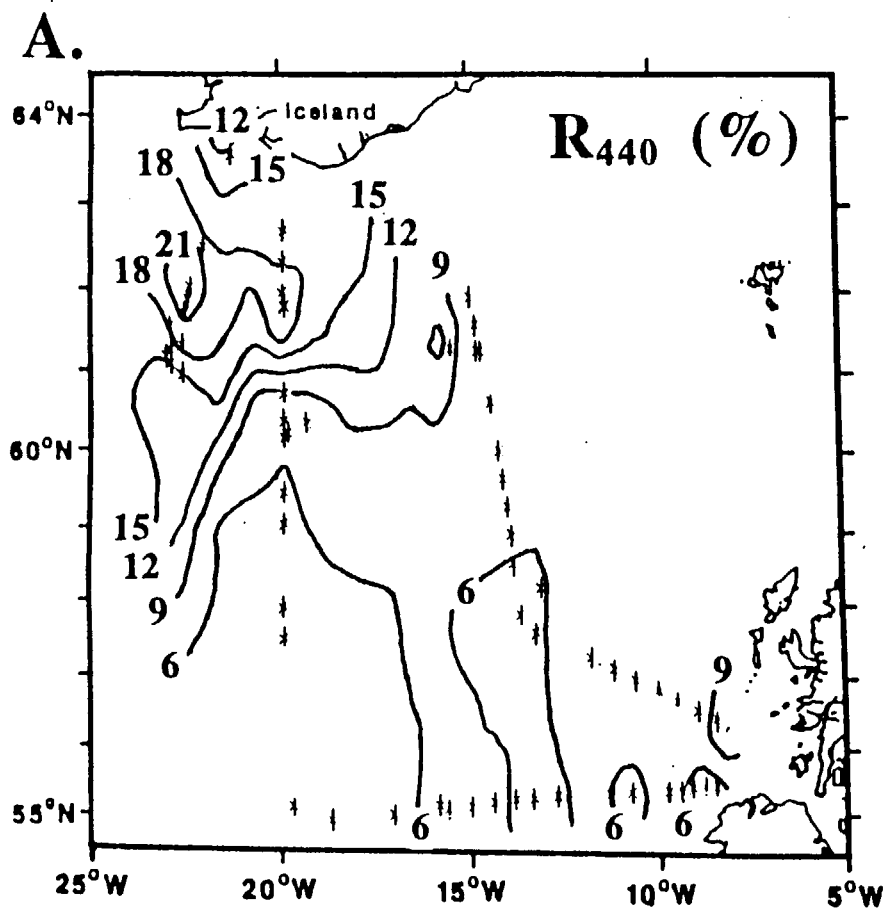


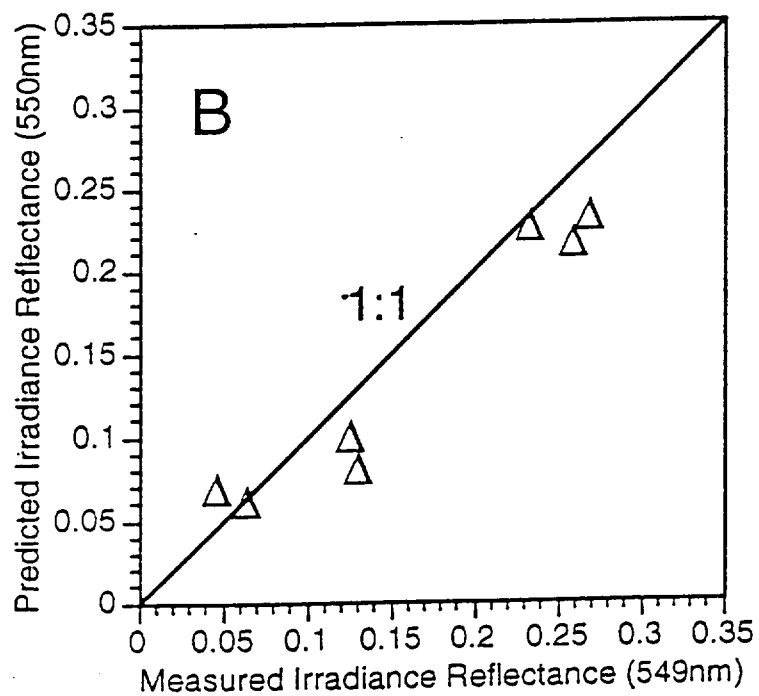
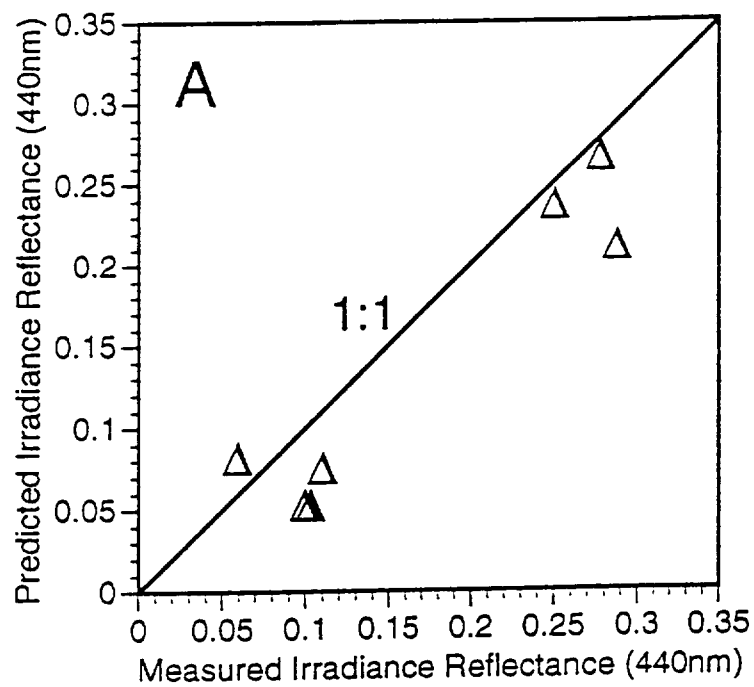






NOAA-11 19 June 1991 15:04 GMT





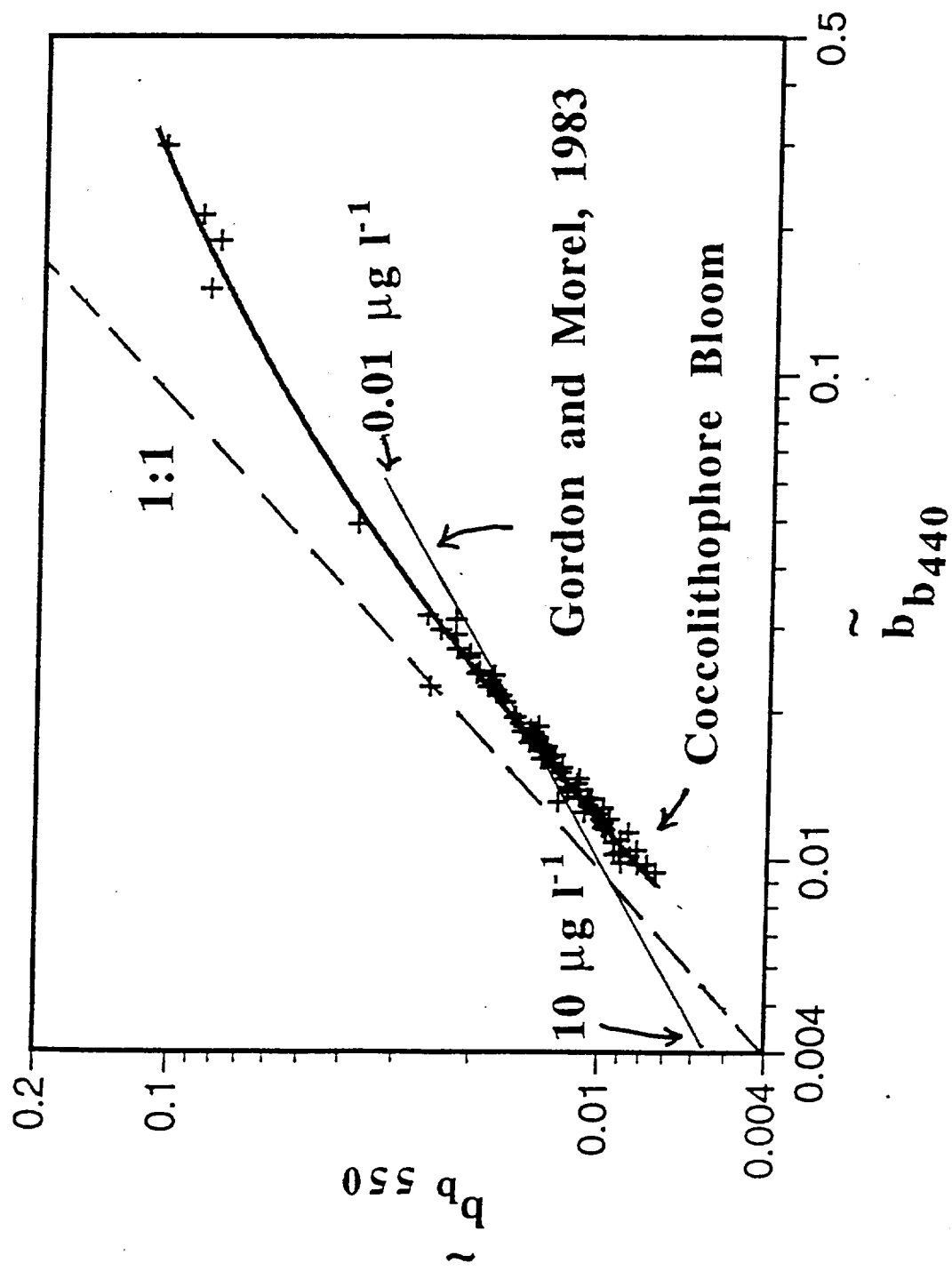


Fig. 11